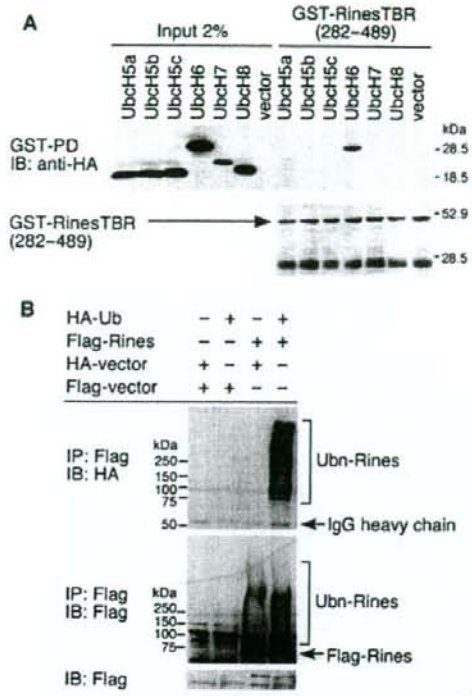

Figure 6 Rines can bind to a ubiquitin-conjugating E2 enzyme and can be polyubiquitinated. (A) Rines binds selectively to UbcH6. Extracts from 293T cells expressing the ubiquitin-conjugating E2 enzymes (Myc-UbcH5a, H5b, H5c, H6, H7, H8) were subjected to GST pull-down assay using the GST-Rines-TBR fusion product, and detected with anti-Myc antibody (*upper panel*). GST-Rines-TBR fusion product was shown as amido black staining (*lower panel*). (B) Rines is polyubiquitinated in NIH 3T3 cells. NIH 3T3 cells were transfected with the plasmids indicated. An equal amount of protein from each cell lysate was immunoprecipitated with anti-Flag antibody and then immunoblotted with anti-HA or anti-Flag antibodies to detect ubiquitinated proteins as smear bands (*upper two panels*). Expression analysis of Flag-Rines by immunoblotting of cell extracts (*bottom panel*). The protein ratio used for the immunoprecipitation and immunoblotting lanes was 65 : 1.

2000; Pickart 2001), these results support the hypothesis that Rines is an E3 ubiquitin ligase. In addition, we observed the interaction of endogenous Zic2 with both Myc-Rines and Myc-ΔRING (Fig. 7B) in the immunoprecipitation assay. This result is consistent with the *in vitro* binding to Zic2 by Rines (Fig. 4C,D) and the co-immunoprecipitation of Rines with Zic2 (Fig. 5A). These results suggest that Rines can promote the ubiquitination of the interacting protein.

Discussion

Rines gene-encoded product is a novel member of the RING finger protein family and functions as an E3 ubiquitin ligase

Rines contained two functional domains, a C3HC4-type RING finger domain and a basic coiled-coil domain, both of which can act as protein binding domain. As with many other RING-type E3 ligases, the RING finger motif of Rines may function as a recruiting motif for an E2 ubiquitin-conjugating enzyme, UbcH6, because Rines-TBR, which contains the RING finger motif, can bind UbcH6. In addition, the RING finger motif of Rines is required for its protein ubiquitination activity. These results support the inference that Rines functions as an E3 ubiquitin ligase. The coiled-coil domain is known to participate in homo-multimerization of proteins and protein–protein interaction (Jensen *et al.* 2001; Reymond *et al.* 2001). Interestingly, co-existence of the RING domain and the coiled-coil domain is also found in RBCC/TRIM proteins, the RING finger domain of which is similar to that of Rines (Fig. 1C), and in which coiled-coil domains play a role in homo-multimerization and the cell compartment-specific distribution of proteins (Reymond *et al.* 2001; Dho & Kwon 2003). In addition, co-existence of the RING domain and the coiled-coil domain was reported in Staring, which is an E3 ubiquitin ligase targeting syntaxin (Chin *et al.* 2002). In this case, the coiled-coil domain acts as the substrate-binding domain. The finding that the coiled-coil domain can bind a protein is consistent with the macromolecular assembling properties of this domain.

As to the molecular function of Rines, we revealed that Rines functions as an E3 ubiquitin ligase on the basis of the following three facts: (i) Flag-Rines promote the proteasomal degradation of the interacting protein, (ii) Myc-Rines enhance the ubiquitination of the interacting protein, and (iii) GST-Rines-TBR associates with an E2 ubiquitin-conjugating enzyme (Myc-UbcH6). Furthermore, Flag-Rines itself is heavily ubiquitinated and degraded by proteasome as are the case in many other E3 ubiquitin ligase (Fang & Weissman 2004). A rapid degradation of Flag-Rines itself was also observed in cycloheximide chase experiments. This may explain why we could not detect endogenous Rines protein in brain lysates by using anti-Rines antibodies, which could detect over-expressed Rines in cultured cells treated with a proteasome inhibitor (data not shown).

In terms of other molecular properties of Rines, its location in the ER membrane is intriguing. Recent studies of the ER-associated protein degradation (ERAD)

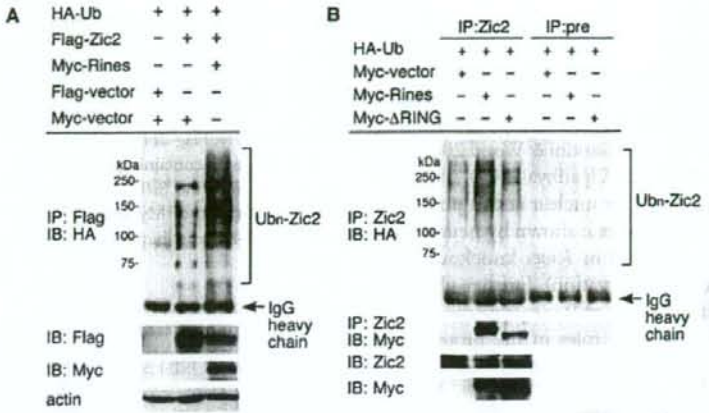

Figure 7 Rines shows ubiquitin-ligase activity. (A) NIH 3T3 cells were transfected with the plasmids indicated. An equal amount of protein from each cell lysate was immunoprecipitated with anti-Flag antibody and then immunoblotted with anti-HA antibody to detect ubiquitinated proteins as smear bands (*upper panel*). Expression analysis of Flag- and Myc-tagged gene products and actin protein, respectively, by immunoblotting of cell extracts (*bottom three panels*). The protein ratio used for the immunoprecipitation and immunoblotting lanes was 30 : 1. (B) Rines promotes the ubiquitination of endogenous protein in a RING finger domain-dependent manner. MNS70 cells were transfected with the plasmids indicated and cultured with a proteasome inhibitor (epoxomicin). An equal amount of protein from each cell lysate was immunoprecipitated with anti-Zic2 antibody and then immunoblotted with anti-HA antibody to detect ubiquitinated Zic2 (*top panel*) and with anti-Myc antibody to detect the interaction of Zic2 and Rines (*second from the top panel*). Zic2 protein and Myc-tagged Rines in the cell extracts were confirmed by immunoblotting (*bottom two panels*). The protein ratio used for the immunoprecipitation and immunoblotting lanes was 10 : 1.

system have shown that this system is an essential protein proofreading and elimination system (Kostova & Wolf 2003). Studies in yeast have shown that the RING-finger-domain-containing ER integral membrane proteins Der3/Hrd1p and Doa10 cooperate with an E2 ubiquitin-conjugating enzyme, and they are considered to act as E3 ubiquitin ligases in the ERAD pathway (Bays *et al.* 2001; Deak & Wolf 2001; Swanson *et al.* 2001; Deng & Hochstrasser 2006; Ravid *et al.* 2006). Moreover, RING-finger-domain-containing ER membrane proteins, gp78 and RMA1, are considered to be the mammalian orthologs of the yeast ERAD machinery (Fang *et al.* 2001; Younger *et al.* 2006). The RBCC/TRIM protein RFP2 was recently reported to be an ER membrane-anchored ubiquitin ligase involved in the ERAD pathway (Lerner *et al.* 2007). However, it is possible that additional functional homologues exist in vertebrates, considering the increased diversity of functional proteins in vertebrates compared with in yeast. Rines may be a good candidate for a component of the ERAD system in the vertebrate CNS. It is known that Doa10, which resides in the ER/nuclear envelope, degrades the nuclear transcription factor Matα2 as well as ER proteins (Swanson *et al.* 2001; Deng & Hochstrasser 2006; Ravid *et al.* 2006). It is possible that Rines can act in a similar fashion to Doa10 and degrade the substrates of the ERAD pathway as well as nuclear proteins. This possibility should be addressed in a future study.

Possible biological roles of Rines

By using Zic2 as a tool protein that can bind Rines, we demonstrated the proteasomal degradation activity of Rines. However, the biological significance of Rines-mediated Zic2-degradation *in vivo* is unclear, because we did not see a clear increase in Zic2 protein amount in conventional immunoblot or immunofluorescence staining analyses of the brains of *Rines* knockout mice (M.O., J.A. unpublished observation). Although we cannot exclude the possibility that Rines-mediated Zic2 degradation occurs occasionally, it seems better to postulate that there are other major degradation targets of Rines *in vivo*.

Since the expression of *Rines* is strong in immature neural cells and lens cells, we are interested in the possible degradation targets of Rines in these tissues. In addition, the role of Rines in the mature brain, another major organ showing *Rines* expression, should be clarified,

taking into account emerging roles of the ubiquitin–proteasome pathway in the modulation of neuronal function, such as regulation of synaptic structure and synaptic plasticity (Johnston & Madura 2004; Moriyoshi *et al.* 2004; Yao *et al.* 2007) and in neurodegeneration, such as in Parkinson's disease (Gandhi & Wood 2005) and Alzheimer's disease (Hegde & Upadhya 2007). Although the authentic Rines targets are unclear at this point, the biological significance of Rines is shown by neurobehavioral abnormalities observed in *Rines* knockout mice (M.O., J.A. unpublished observation). Further clarification of the molecular function of Rines is needed for an in-depth understanding of its roles in the proteasomal degradation system in mammalian brains.

Experimental procedures

Yeast two-hybrid screening

Yeast two-hybrid screening was done according to (Mizugishi *et al.* 2004) using an amino-terminal region of mouse Zic2 (amino acid number 1–255) as a bait protein.

cDNA cloning and plasmid construction

Full-length mouse *Rines* cDNA (accession: AAH46775) was cloned by using cDNA library screening and PCR. The cDNA fragment from a cDNA clone obtained in the two-hybrid screening was used for the screening of mouse cerebellum λ-gt11 cDNA library (gifted by Dr T. Furuichi). We obtained the partial cDNA fragment of the *Rines* gene by the screening. Then, 5′ end of the mouse *Rines* cDNA was cloned from E15 mouse embryonic brain cDNAs by using the PCR. The primers used were 5′-TAG CAGCTAATCTCGGTTGC-3′, derived from NCBI database accession: AK013941 and, 5′-GGACATGCACTGATCAGTAA-3′, derived from the cDNA fragment obtained by library screening. The PCR conditions were 35 cycles of 94 °C for 15 min, 58 °C for 1 min and 72 °C for 2 min. The expression vector Flag-Rines was constructed by inserting the entire protein-coding region of *Rines* in-frame into the AviII/SrfI-EcoRI site of pCMVtag2 (Stratagene, La Jolla, CA).

To express Flag-tagged, hemagglutinin (HA)-tagged, and Myc-tagged gene products, the relevant sequences were amplified by PCR, verified by DNA sequencing, and subcloned into pCMVtag2 (Stratagene), pcDNA3HA (a gift from Dr T. Nakajima), and pCS2 + MT (Turner & Weintraub 1994). For the Myc-Rines construct, full-length *Rines* (1–591) was amplified by PCR and digested with *Eco*RI into pCS2 + MT. In the case of Rines-ΔRING-(431–472), two fragments (1–430 and 473–591) amplified by PCR were digested with *Xho*I-*Bgl*I and *Bgl*I-*Xho*I, joined together, and then inserted into pCS2 + MT. The GST-Zic2 was constructed by inserting the cDNA fragment containing the entire ORF of mouse Zic2 into the EcoRI site of pGEX-4T3 vector (Pharmacia, Saclay, France). For the GST-Rines-deletions constructs, fragments were amplified by PCR using primers that contain BamHI-EcoRI sites, sequenced, and cloned into the BamHI- EcoRI sites of the pGEX-4T1 vector (Pharmacia).

HA-Zic2 and Flag-Zic2 were constructed by inserting the cDNA fragment containing the entire ORF of mouse Zic2 into the BamHI-EcoRI site of pcDNA3HA or pCMVtag2 (Mizugishi *et al.* 2001). The Flag-2HA-Zic2 was constructed by inserting the cDNA fragment containing the two tandem repeat of hemagglutinin (HA) into the SrfI-BamHI site of pCMVtag2-Flag-Zic2. The construction of Myc-tagged UbcH5a, H5b, H5c, H6, H7, H8 and HA-tagged Ubiquitin expression vectors will be described elsewhere.

Cell culture and transfection

293T, COS7 and NIH 3T3 cells were maintained at 37 °C with 5% CO_2 in Dulbecco's Modified Eagle's Medium (DMEM, Sigma, St Louis, MO) supplemented with 10% fetal bovine serum (FBS). MNS70 cells (rat neural stem-derived cells, Nakagawa *et al.* 1996) were maintained at 37 °C with 5% CO_2 in a 1 : 1 mixture of DMEM and F12 medium (DF, Sigma) supplemented with 10% FBS, 5% horse serum (HS), and antibiotics. The cells were plated at a density of 3.5×10^4 cells/cm^2 24 h before transfection. 293T and COS7 cells were transfected with Effectene transfection reagent (Qiagen, Valencia, CA) or Trans-IT-LT1 transfection reagent (Mirus, Madison, WI), NIH 3T3 cells were transfected with Superfect transfection reagent (Qiagen) or Lipofectamine Plus or 2000 transfection reagent (Invitrogen, Carlsbad, CA), and MNS70 cells were transfected with Fugene HD transfection reagent (Roche, Basel, Switzerland), according to the manufacturer's instructions.

Immunoblotting

The proteins and gene products were separated by 7.5%–15% SDS-polyacrylamide gel electrophoresis and transferred to PVDF membrane (Immobilon, Millipore, Bedford, MA). The membranes were immersed in 3%–6% skim milk overnight at 4 °C and incubated with first antibody. The bound antibodies were detected using horseradish peroxidase-conjugated secondary antibodies (anti-mouse, rabbit or rat IgG) and ECL reagents (Amersham Pharmacia Biotech, Uppsala, Sweden).

Subcellular localization studies

COS7 cells were transiently transfected with Flag-Rines. Cells were fixed at 24 h after transfection in 4% paraformaldehyde in 0.1 M sodium phosphate buffer for 15 min at room temperature, incubated with blocking buffer (5% bovine serum albumin in phosphate-buffered saline) for 1 h at room temperature and then incubated overnight at 4 °C with the anti-Calnexin antibody (Stressgen, San Diego, CA) and anti-Flag M2 monoclonal antibody (Sigma) diluted with buffer (0.3% triton X-100 and 1% bovine serum albumin in phosphate-buffered saline). The bound antibodies were detected by Alexa 488-conjugated anti-mouse IgG or Alexa 594-conjugated anti-rabbit IgG antibodies (Molecular Probes Inc., Eugene, OR).

Membrane preparation and protease protection assay

The membrane fraction was prepared as described (Lenk *et al.* 2002). For microsomes of Flag-Rines-transfected 293T cells, cells were scraped 24 h after transfection and then washed once in PBS and homogenized in a homogenization buffer (50 mM Tris–HCl, pH 7.5, 250 mM sucrose, 2 mM EDTA, 150 mM KCl, 1 mM DTT and complete protease inhibitor cocktail (Roche)). The cell lysates were centrifuged at 3000 *g* for 10 min at 4 °C. After centrifugation at 10 000 *g* for 15 min, the supernatant was subsequently centrifuged at 75 000 *g* for 60 min and the pellet (microsome fraction) was resuspended in a membrane buffer (150 mM sucrose, 50 mM Hepes, pH 7.5, 2.5 mM MgOAc, 50 mM KOAc and protease inhibitors) or a membrane buffer containing 2.5 M Urea, 800 mM KOAc, 0.1 M Na_2CO_3, 500 mM NaCl or 2% sodium deoxycholate or TNE buffer (150 mM Tris–HCl, pH 7.5, 500 mM NaCl, 1 mM EDTA, 1% Triton X-100, 0.1% SDS). The cell suspensions were centrifuged at 18 000 *g* for 60 min, then the pellets were resuspended in preboiled SDS-lysis buffer (50 mM Tris–HCl, pH 7.5, 0.5 mM EDTA, 1% SDS, 1 mM dithiothreitol), boiled for an additional 10 min and diluted 10-fold by adding 0.5% NP-40 buffer. A protease protection assay was performed according to the method of Sommer and Jentsch (1993). Myc-Rines-transfected 293T cells were homogenized in the homogenization buffer without EDTA or protease inhibitor and then centrifuged at 3000 *g* for 10 min at 4 °C. The crude homogenates were treated with protease K (20 μg/mL), or untreated, in the presence or absence of detergent buffer (TNE). The following antibodies were used in this study: anti-Flag (M2, Sigma), anti-Myc (9E10, Santa Cruz Biotechnology), anti-Calnexin (BD Biosciences, La Jolla, CA), anti-Calreticulin (BD Biosciences), anti-TRAPα (Upstate, Lake Placid, NY), anti-KDEL (Stressgen).

Northern blot analysis

Two types of Northern blot sheets (Mouse Adult Tissue Blot, Mouse Embryo Full Stage Blot, Seegene, Seoul, Korea) were used to determine the expression profiles of the mouse *Rines* genes. ^{32}P-labeled Rines cDNA probe corresponding to the 1.1 kb fragment of Rines cDNA, from the last RING finger motif toward the 3′untranslated region was synthesized with Random Primed DNA Labeling Kit (Roche). The hybridizations were performed in a buffer consisting of 0.5 M Na_2HPO_4, pH7.2, 7.0% SDS, 1% BSA, 1 mM EDTA, pH8.0, 100 μg/mL herring sperm DNA at 65 °C overnight. These membranes were washed 3 times with 2 × SSC-0.1% SDS at room temperature for 5 min, and finally washed with 0.1 × SSC-0.1% SDS at 56 °C for 40 min, and X-ray films were exposed to the washed membrane with an intensifying screen for 24 h to 7 days. The images were digitized, and the contrast and brightness were optimized.

In situ hybridization

The expression of the *Rines* in the developing animal was investigated in ICR mice purchased from Nihon SLC (Shizuoka, Japan). All animal experiments were carried out according to the guidelines for animal experimentation in RIKEN. *In situ* hybridizations were performed was done as previously described (Nagai *et al.* 1997). Same probe for *Rines* in the Northern blot analysis was used. The specificity of the hybridization signals was verified by the absence of any signals in a control hybridization performed with a *Zic2* sense-strand probe (Nagai *et al.* 1997).

GST pull-down assay

Flag-2HA-Zic2 was purified from 293T cells that were transiently transfected with pCMV-Flag-2HA-Zic2 (Ishiguro *et al.* 2007). Produced protein was affinity-purified with anti-HA agarose beads (Sigma) and HA-peptide (100 ng/mL, Sigma), followed by subsequent affinity purification using anti-Flag agarose beads (Sigma) and Flag-peptide (100 ng/mL, Sigma).

293T cells were transiently transfected with Flag-Rines, Flag-Zic2 or Myc-ubiquitin-conjugating E2 enzyme expression vectors. Cells were harvested 24 h after transfection and were lysed in an immunoprecipitation buffer A (25 mM Hepes, pH 7.2, 0.5% NP-40, 150 mM NaCl, 50 mM NaF, 2 mM Na_3VO_4, 1 mM phenylmethylsulfonyl fluoride, and 20 μg/mL aprotinin) or buffer B (20 mM Hepes, pH 7.4, 150 mM NaCl, 5 mM EDTA, 10% glycerol, 0.5% Triton X-100, 0.5 mM N-ethylmaleimide, 0.5 mM iodoacetamide, 1 mM phenylmethylsulfonyl fluoride and 20 μg/mL aprotinin and contained with 0.1 mg/mL BSA in the case of the direct binding assay). After a centrifugation at 15 000 *g* for 15 min, these supernatant and Flag-2HA-Zic2 were incubated for 2 h at 4 °C with appropriate GST-fusion proteins, and then added with 20 μL of 50% suspension of Glutathione Sepharose 4B beads and incubated for another 2 h at 4 °C. After washing 5 times with the same immunoprecipitation buffer, bound proteins were separated by SDS-PAGE, immunoblotted with the anti-Flag M2 monoclonal antibody (Sigma) or anti-HA Y-11 polyclonal antibody (Santa Cruz Biotechnology, Santa Cruz, CA), or anti-HA 3F10 rat monoclonal antibody (Roche), and detected by ECL system (Amersham, Uppsala, Sweden).

Immunoprecipitation assay

293T cells were transfected with HA-Zic2 and Flag-Rines or Flag-tagged vector. 48 h after transfection, the cells were treated with the proteasome inhibitor MG132 (Carbobenzoxy-Leu-Leu-Leu-CHO, 20 μM; Calbiochem, San Diego, CA), E64 (50 μM; Sigma) or vehicle Me_2SO; DMSO (final concentration (0.2%)) for 12 h. Cells were then lysed in the immunoprecipitation buffer A (described above) and the lysate was centrifuged at 15 000 *g* for 15 min. These supernatant were incubated for 2 h at 4 °C with a 23 μg of anti-Flag M2 monoclonal antibody (Sigma), and then incubated for another 2 h at 4 °C after adding 20 μL of 50% suspension of protein G agarose beads (Pierce). After washing 5 times with the buffer A, the bound proteins were analyzed by SDS-PAGE and immunoblotting as described above.

Degradation assay

NIH 3T3 cells were transfected with HA-Zic2 and Flag-Rines or Flag-tagged control vector. Cells were treated 43 h after transfection

with the proteasome inhibitor, MG132 (10 μM), Epoxomicin (10 μM; Boston Biochem, Cambridge, MA), clasto-Lactacystin-β-lactone (10 μM; BostonBiochem), Lactacystin (20 μM; BostonBiochem or PeptideInstitute, Osaka, Japan), ALLN (Ac-Leu-Leu-Nle-CHO (MG101), 25 μM; Calbiochem), the calpain inhibitor, Calpastatine peptide (1 μM; Calbiochem) or vehicle (DMSO, at a final concentration of 0.2%) for 9 h. The cell lysates were subjected for immunoblotting.

Cycloheximide chase assay

NIH 3T3 cells were transiently co-transfected with HA-Zic2 and Flag-Rines or Flag-tagged vector as described in a degradation assay. 26 h after transfection, culture medium was replaced by DMEM with 10% FBS containing cycloheximide (25 μg/mL). Cells were washed and harvested with PBS(–) buffer 0, 2, 4, 6 h after addition of cycloheximide, lysed and followed by immunoblotting. HA-Zic2 bands and actin bands were densitometrically quantified with NIH Image (v1.61, <http://rsb.info.nih.gov/nih-image/>), and HA-Zic2 amounts were normalized to actin amounts at each time point.

In vivo ubiquitination assay

NIH 3T3 cells were transfected with combinations of the following plasmids: HA-ubiquitin, Flag-Rines, Flag-Zic2, Myc-Rines and Flag-, HA-, Myc-tagged control vectors. After 50 h of incubation, the cells were lysed in a lysis buffer (20 mM Hepes, pH 7.4, 150 mM NaCl, 5 mM EDTA, 10% glycerol, 0.5% Triton X-100, 0.5 mM *N*-ethylmaleimide, 0.5 mM iodoacetamide, and 5 nM ubiquitin aldehyde (Calbiochem)) and a complete protease inhibitor cocktail (Roche). The lysates were subjected to immunoprecipitation by using anti-Flag agarose beads (18 μL, Sigma) and to an immunoblot analysis with anti-HA antibody (Roche) or anti-Flag antibody. For the endogenous Zic2 ubiquitination assay, MNS70 cells were transfected with combinations of the following plasmids: HA-ubiquitin, Myc-Rines, Myc-ΔRING, and Myc-tagged control vector. Forty-three hours after transfection, the cells were incubated for 6 h with 5 μM epoxomicin. The cells lysed in the lysis buffer described above, and the lysates were subjected to immunoprecipitation with anti-Zic2 antibody and immunoblot analysis with anti-HA antibody (Roche).

Acknowledgements

We thank Haruhiko Bito for critical comments on manuscript, Takashi Inoue, Kei-ichi Katayama, Naoko Morimura and Takahiko J Fujimi for technical advice and helpful discussions, members of Aruga and Mikoshiba laboratories for helpful discussions and Shigetsugu Hatakeyama for the gift of HA-ubiquitin vector. This work is supported in parts by The Mochida Memorial Foundation of Medical Pharmaceutical Research, and Grants-in-Aid for Scientific Research from Ministry of Education, Culture, Sports, Science and Technology of Japan.

References

Aruga, J., Nagai, T., Tokuyama, T., Hayashizaki, Y., Okazaki, Y., Chapman, V.M. & Mikoshiba, K. (1996) The mouse zic gene family. Homologues of the *Drosophila* pair-rule gene odd-paired. *J. Biol. Chem.* **271**, 1043–1047.

Bays, N.W., Gardner, R.G., Seelig, L.P., Joazeiro, C.A. & Hampton, R.Y. (2001) Hrd1p/Der3p is a membrane-anchored ubiquitin ligase required for ER-associated degradation. *Nat. Cell Biol.* **3**, 24–29.

Borden, K.L. (2000) RING domains: master builders of molecular scaffolds? *J. Mol. Biol.* **295**, 1103–1112.

Chin, L.S., Vavalle, J.P. & Li, L. (2002) Staring, a novel E3 ubiquitin–protein ligase that targets syntaxin 1 for degradation. *J. Biol. Chem.* **277**, 35071–35079.

Deak, P.M. & Wolf, D.H. (2001) Membrane topology and function of Der3/Hrd1p as a ubiquitin–protein ligase (E3) involved in endoplasmic reticulum degradation. *J. Biol. Chem.* **276**, 10663–10669.

Deng, M. & Hochstrasser, M. (2006) Spatially regulated ubiquitin ligation by an ER/nuclear membrane ligase. *Nature* **443**, 827–831.

Dho, S.H. & Kwon, K.S. (2003) The Ret finger protein induces apoptosis via its RING finger-B box-coiled-coil motif. *J. Biol. Chem.* **278**, 31902–31908.

Eto, A., Akita, Y., Saido, T.C., Suzuki, K. & Kawashima, S. (1995) The role of the calpain–calpastatin system in thyrotropin-releasing hormone-induced selective down-regulation of a protein kinase C isozyme, nPKCε, in rat pituitary GH4C1 cells. *J. Biol. Chem.* **270**, 25115–25120.

Fang, S. & Weissman, A.M. (2004) A field guide to ubiquitylation. *Cell Mol. Life Sci.* **61**, 1546–1561.

Fang, S., Ferrone, M., Yang, C., Jensen, J.P., Tiwari, S. & Weissman, A.M. (2001) The tumor autocrine motility factor receptor, gp78, is a ubiquitin protein ligase implicated in degradation from the endoplasmic reticulum. *Proc. Natl. Acad. Sci. USA* **98**, 14422–14427.

Fujiki, Y., Hubbard, A.L., Fowler, S. & Lazarow, P.B. (1982) Isolation of intracellular membranes by means of sodium carbonate treatment: application to endoplasmic reticulum. *J. Cell Biol.* **93**, 97–102.

Gandhi, S. & Wood, N.W. (2005) Molecular pathogenesis of Parkinson's disease. *Hum Mol. Genet* **14**, 2749–2755.

Giaever, G., Chu, A.M., Ni, L., *et al.* (2002) Functional profiling of the *Saccharomyces cerevisiae* genome. *Nature* **418**, 387–391.

Hegde, A.N. & Upadhya, S.C. (2007) The ubiquitin–proteasome pathway in health and disease of the nervous system. *Trends Neurosci.* **30**, 587–595.

Hershko, A. & Ciechanover, A. (1998) The ubiquitin system. *Annu. Rev. Biochem.* **67**, 425–479.

Hirokawa, T., Boon-Chieng, S. & Mitaku, S. (1998) SOSUI: classification and secondary structure prediction system for membrane proteins. *Bioinformatics* **14**, 378–379.

Ishiguro, A., Ideta, M., Mikoshiba, K., Chen, D.J. & Aruga, J. (2007) Zic2-dependent transcriptional regulation is mediated by DNA-dependent protein kinase, poly(ADP-ribose) polymerase and RNA helicase A. *J. Biol. Chem.* **282**, 9983–9995.

Jensen, K., Shiels, C. & Freemont, P.S. (2001) PML protein isoforms and the RBCC/TRIM motif. *Oncogene* **20**, 7223–7233.

Joazeiro, C.A. & Weissman, A.M. (2000) RING finger proteins: mediators of ubiquitin ligase activity. *Cell* **102**, 549–552.

Johnston, J.A. & Madura, K. (2004) Rings, chains and ladders: ubiquitin goes to work in the neuron. *Prog Neurobiol* **73**, 227–257.

Kostova, Z. & Wolf, D.H. (2003) For whom the bell tolls: protein quality control of the endoplasmic reticulum and the ubiquitin–proteasome connection. *EMBO J.* **22**, 2309–2317.

Lenk, U., Yu, H., Walter, J., Gelman, M.S., Hartmann, E., Kopito, R.R. & Sommer, T. (2002) A role for mammalian Ubc6 homologues in ER-associated protein degradation. *J. Cell Sci.* **115**, 3007–3014.

Lerner, M., Corcoran, M., Cepeda, D., Nielsen, M.L., Zubarev, R., Ponten, F., Uhlen, M., Hober, S., Grander, D. & Sangfelt, O. (2007) The RBCC gene RFP2 (Leu5) encodes a novel transmembrane E3 ubiquitin ligase involved in ERAD. *Mol. Biol. Cell* **18**, 1670–1682.

Mizugishi, K., Aruga, J., Nakata, K. & Mikoshiba, K. (2001) Molecular properties of Zic proteins as transcriptional regulators and their relationship to GLI proteins. *J. Biol. Chem.* **276**, 2180–2188.

Mizugishi, K., Hatayama, M., Tohmonda, T., Ogawa, M., Inoue, T., Mikoshiba, K. & Aruga, J. (2004) Myogenic repressor I-mfa interferes with the function of Zic family proteins. *Biochem. Biophys. Res. Commun.* **320**, 233–240.

Moriyoshi, K., Iijima, K., Fujii, H., Ito, H., Cho, Y. & Nakanishi, S. (2004) Seven in absentia homolog 1A mediates ubiquitination and degradation of group 1 metabotropic glutamate receptors. *Proc. Natl. Acad. Sci. USA* **101**, 8614–8619.

Munoz-Alonso, M.J., Guillemain, G., Kassis, N., Girard, J., Burnol, A.F. & Leturque, A. (2000) A novel cytosolic dual specificity phosphatase, interacting with glucokinase, increases glucose phosphorylation rate. *J. Biol. Chem.* **275**, 32406–32412.

Nagai, T., Aruga, J., Minowa, O., Sugimoto, T., Ohno, Y., Noda, T. & Mikoshiba, K. (2000) Zic2 regulates the kinetics of neurulation. *Proc. Natl. Acad. Sci. USA* **97**, 1618–1623.

Nagai, T., Aruga, J., Takada, S., Gunther, T., Sporle, R., Schughart, K. & Mikoshiba, K. (1997) The expression of the mouse Zic1, Zic2, and Zic3 gene suggests an essential role for Zic genes in body pattern formation. *Dev Biol.* **182**, 299–313.

Nakagawa, Y., Kaneko, T., Ogura, T., Suzuki, T., Torii, M., Kaibuchi, K., Arai, K., Nakamura, S. & Nakafuku, M. (1996) Roles of cell-autonomous mechanisms for differential expression of region-specific transcription factors in neuroepithelial cells. *Development* **122**, 2449–2464.

Pickart, C.M. (2001) Mechanisms underlying ubiquitination. *Annu. Rev. Biochem.* **70**, 503–533.

Ravid, T., Kreft, S.G. & Hochstrasser, M. (2006) Membrane and soluble substrates of the Doa10 ubiquitin ligase are degraded by distinct pathways. *EMBO J.* **25**, 533–543.

Reymond, A., Meroni, G., Fantozzi, A., Merla, G., Cairo, S., Luzi, L., Riganelli, D., Zanaria, E., Messali, S., Cainarca, S., Guffanti, A., Minucci, S., Pelicci, P.G. & Ballabio, A. (2001) The tripartite motif family identifies cell compartments. *EMBO J.* **20**, 2140–2151.

Rost, B., Fariselli, P. & Casadio, R. (1996) Topology prediction for helical transmembrane proteins at 86% accuracy. *Protein Sci.* **5**, 1704–1718.

Sommer, T. & Jentsch, S. (1993) A protein translocation defect linked to ubiquitin conjugation at the endoplasmic reticulum. *Nature* **365**, 176–179.

Strausberg, R.L., Feingold, E.A., Grouse, L.H., *et al.* (2002) Generation and initial analysis of more than 15 000 full-length human and mouse cDNA sequences. *Proc. Natl. Acad. Sci. USA* **99**, 16899–16903.

Swanson, R., Locher, M. & Hochstrasser, M. (2001) A conserved ubiquitin ligase of the nuclear envelope/endoplasmic reticulum that functions in both ER-associated and Matα2 repressor degradation. *Genes Dev.* **15**, 2660–2674.

Turner, D.L. & Weintraub, H. (1994) Expression of achaete-scute homolog 3 in *Xenopus* embryos converts ectodermal cells to a neural fate. *Genes Dev.* **8**, 1434–1447.

Yao, I., Takagi, H., Ageta, H., *et al.* (2007) SCRAPPER-dependent ubiquitination of active zone protein RIM1 regulates synaptic vesicle release. *Cell* **130**, 943–957.

Younger, J.M., Chen, L., Ren, H.Y., Rosser, M.F., Turnbull, E.L., Fan, C.Y., Patterson, C. & Cyr, D.M. (2006) Sequential quality-control checkpoints triage misfolded cystic fibrosis transmembrane conductance regulator. *Cell* **126**, 571–582.

Received: 19 September 2007
Accepted: 10 January 2008

Author Query Form

Journal: Genes to Cells

Article: gtc_1169.fm

Dear Author,

During the copy-editing of your paper, the following queries arose. Please respond to these by marking up your proofs with the necessary changes/additions. Please write your answers on the query sheet if there is insufficient space on the page proofs. Please write clearly and follow the conventions shown on the attached corrections sheet. If returning the proof by fax do not write too close to the paper's edge. Please remember that illegible mark-ups may delay publication.

Many thanks for your assistance.

No.	Query	Remarks
1	Author: Please expand the authors name.	
2	Author: Please confirm the locations of manufacturers that are inserted.	
3	Author: All gene names should be in italics and proteins should be in roman. Please check.	

The EMBO Journal (2008) 27, 2432–2443 | © 2008 European Molecular Biology Organization | All Rights Reserved 0261-4189/08
www.embojournal.org

THE EMBO JOURNAL

Phosphorylation of 4E-BP by LRRK2 affects the maintenance of dopaminergic neurons in *Drosophila*

Yuzuru Imai[1,*], Stephan Gehrke[2,3], Hua-Qin Wang[4], Ryosuke Takahashi[4], Kazuko Hasegawa[5], Etsuro Oota[6] and Bingwei Lu[2,3,*]

[1]Institute of Development, Aging and Cancer, Tohoku University, Sendai, Japan, [2]Department of Pathology, Stanford University School of Medicine, Palo Alto, CA, USA, [3]GRECC/VAPAHCS, Palo Alto, CA, USA, [4]Department of Neurology, Kyoto University Graduate School of Medicine, Kyoto, Japan, [5]Department of Neurology, Sagamihara National Hospital, National Hospital Organization, Sagamihara, Japan and [6]Division of Clinical Immunology, Kitasato University Graduate School of Medical Science, Sagamihara, Japan

Dominant mutations in leucine-rich repeat kinase 2 (LRRK2) are the most frequent molecular lesions so far found in Parkinson's disease (PD), an age-dependent neurodegenerative disorder affecting dopaminergic (DA) neuron. The molecular mechanisms by which mutations in LRRK2 cause DA degeneration in PD are not understood. Here, we show that both human LRRK2 and the *Drosophila* orthologue of LRRK2 phosphorylate eukaryotic initiation factor 4E (eIF4E)-binding protein (4E-BP), a negative regulator of eIF4E-mediated protein translation and a key mediator of various stress responses. Although modulation of the eIF4E/4E-BP pathway by LRRK2 stimulates eIF4E-mediated protein translation both *in vivo* and *in vitro*, it attenuates resistance to oxidative stress and survival of DA neuron in *Drosophila*. Our results suggest that chronic inactivation of 4E-BP by LRRK2 with pathogenic mutations deregulates protein translation, eventually resulting in age-dependent loss of DA neurons.

The EMBO Journal (2008) **27**, 2432–2443. doi:10.1038/emboj.2008.163; Published online 14 August 2008
Subject Categories: neuroscience; molecular biology of disease
Keywords: 4E-BP; dopaminergic neurodegeneration; LRRK2; Parkinson's disease; protein translation

Introduction

Parkinson's disease (PD) is a neurodegenerative disease that affects the maintenance of dopaminergic (DA) neurons. PD prevalence is estimated at ~1% among people over the age of 65 years and is increased to 5% for people aged 85 years and older. Most PD cases are sporadic, with oxidative stress being one prominent pathological feature (Jenner, 2003). A small percentage of PD cases are inherited in a Mendelian manner, and several disease-causing genes have been identified (Moore *et al*, 2005). Although most of the familial cases are of early onset, mutations in *leucine-rich repeat kinase 2* (*LRRK2*) cause an autosomal-dominant form of familial PD late in life (Paisan-Ruiz *et al*, 2004; Zimprich *et al*, 2004). *LRRK2* encodes a large protein with multiple domains, including GTPase and kinase domains. *LRRK2*-associated familial PD is largely indistinguishable from the more common sporadic PD in clinical and pathological aspects. Among the known familial PD genes, *LRRK2* is most frequently mutated in sporadic cases, suggesting a general involvement of *LRRK2* in PD pathogenesis (Taylor *et al*, 2006). So far, amino-acid substitutions associated with familial PD have been identified within the multiple domains (Mata *et al*, 2006). Some pathogenic mutations in the kinase domain, such as G2019S and I2020T, were shown to cause moderately enhanced kinase activity *in vitro* (West *et al*, 2005; Gloeckner *et al*, 2006). It is not clear whether mutations in other domains (e.g., R1441G and Y1699C) also affect kinase activity. The pathogenic function of LRRK2 mutations and the biochemical pathways involved are unknown. Key to addressing these important questions is the identification of the physiological substrate(s) of LRRK2.

Translational control is critical for early development of most metazoans and for cell survival under various stress (Holcik and Sonenberg, 2005). It allows an organism to quickly respond to physiological or environmental cues by controlling the expression of proteins from existing mRNAs. Although translation can be regulated at multiple steps, control of translation initiation represents a primary regulatory mechanism. The eukaryotic initiation factor 4E (eIF4E) subunit mediates the binding of eIF4F to the 5′ m^7GpppX cap structure of mRNAs (Sonenberg *et al*, 1979; Gingras *et al*, 1999b). The activity of eIF4E is inhibited by eIF4E-binding protein (4E-BP), which sequesters eIF4E from the eIF4F complex (Gingras *et al*, 1999b; Richter and Sonenberg, 2005). *In vivo*, 4E-BP has an important function for survival under starvation stress, oxidative stress and unfolded protein stress, suggesting that control of translation initiation is closely linked to stress and lifespan (Teleman *et al*, 2005; Tettweiler *et al*, 2005; Yamaguchi *et al*, 2008). 4E-BP is regulated by phosphorylation. One pathway known to influence 4E-BP phosphorylation is the target of rapamycin (TOR) pathway, which integrates nutrient availability, growth factors and cellular energy status to control cell growth. Phosphorylation of 4E-BP causes its release from the eIF4E and relieves its inhibitory effect on translation (Gingras *et al*, 2001; Inoki *et al*, 2005). At least six phosphorylation sites have been identified in human 4E-BP1 (h4E-BP1), including

*Corresponding authors. Y Imai, Institute of Development, Aging and Cancer, Tohoku University, 4-1 Seiryo-Machi, Aoba-Ku, Sendai, Miyagi 980-8575, Japan. Tel.: +81 22 717 8490; Fax: +81 22 717 8490; E-mail: yimai@idac.tohoku.ac.jp or B Lu, GRECC/VAPAHCS, 3801 Miranda Ave, Bldg. 100, Palo Alto, CA 94304, USA. Tel.: +650 849 0373; Fax: +650 852 3440; E-mail: bingwei@stanford.edu

Received: 31 March 2008; accepted: 25 July 2008; published online: 14 August 2008

T37, T46, S65, T70, S83 and S112 (Fadden *et al*, 1997; Heesom *et al*, 1998). A sequential phosphorylation of 4E-BP1 in the order of T37/T46 > T70 > S65 has been proposed (Gingras *et al*, 1999a, 2001). Although the regulatory mechanisms involved in 4E-BP phosphorylation are not fully understood, it appears that a combination of perhaps all phosphorylation events is required to dissociate 4E-BP from eIF4E (Gingras *et al*, 2001).

Here, we show that LRRK2 exerts an effect as a regulator of protein translation by phosphorylating 4E-BP at the T37/T46 sites *in vitro* and *in vivo*. These phosphorylation events appear to be functionally important for the *in vivo* pathogenic effects of the mutant *Drosophila* orthologue of LRRK2 (dLRRK) on stress sensitivity and DA neuron survival. Our results suggest a novel molecular mechanism linking deregulated protein translation to stress sensitivity and neurodegeneration in PD.

Results

dLRRK regulates DA neuron function and maintenance

To understand the biological function and pathogenic function of human LRRK2 (hLRRK2), we have used *Drosophila* as a model system. *Drosophila*, which possesses a dopaminergic system regulating locomotor behaviour and has a short lifespan, is particularly suitable for modelling the late-onset PD caused by LRRK2 mutations. A single orthologue of *LRRK2* (referred to as *dLRRK* hereafter) was identified in the *Drosophila* genome. We cloned full-length *dLRRK* cDNA by RT–PCR. It encodes a 2445 amino-acid protein containing the various domains found in hLRRK2. Critical residues disrupted in familial PD are conserved between hLRRK2 and dLRRK (Figure 1A).

To study the biological function of dLRRK, we analysed its gain-of-function (GOF) and loss-of-function (LOF) effects. For GOF analysis, we generated transgenic (Tg) flies expressing wild-type (WT) dLRRK or mutant dLRRK carrying point mutations found in human PD patients (Figure 1B and Supplementary Figure 1). The DA neuron-specific *tyrosine hydroxylase* (*TH*)- and *dopa decarboxylase* (*Ddc*)-*Gal4* drivers, pan-neuronal *elav-Gal4* driver or the ubiquitous *daughterless* (*Da*)-*Gal4* driver were used to direct transgene expression. For LOF analysis, we obtained one P-element insertion line, in which the expression of full-length dLRRK protein is disrupted, as indicated by the lack of detectable full-length dLRRK protein expression (Figure 1B). In addition, there was no detectable expression of a truncated dLRRK (data not shown). By RT–PCR analysis, we determined that the expression levels of the two genes immediately flanking *dLRRK* were not affected in this *dLRRK* (−/−) mutant (Supplementary Figure 2). Mutant animals are viable, but have decreased fertility in females. In addition, malformed abdomen is often observed in females (Figure 1C), especially when nutritional status is compromised at the larval stage. Because mutants with this phenotype show higher sensitivity to various stress and have shortened lifespan, we excluded them in subsequent analyses.

To test whether dLRRK regulates the function and maintenance of DA neurons, we performed immunohistochemical and neurochemical analyses in *Drosophila*. Immunohistochemical analysis using an anti-dLRRK antibody showed that endogenous dLRRK protein expression is fairly ubiquitous in the fly brain (Supplementary Figure 1B and C). Double labelling with TH showed that it is expressed in DA neurons (Supplementary Figure 1M and N). In Tg animals, we estimated that exogenous WT and mutant dLRRK were expressed at 1.5- to 2.6-fold of endogenous level in TH+ neurons (Supplementary Figure 1M). At the cellular level, endogenous dLRRK was localized in a punctate pattern in the cytoplasmic part of the cell bodies and neurites (Supplementary Figure 1L). Transgenic WT and mutant dLRRK proteins derived from the transgenes were also localized to vesicular structures that co-stain with endosomal markers and partially overlap with synaptic vesicle markers (Supplementary Figure 1H–K and O–V).

In Tg flies expressing PD-related mutant dLRRK, brain dopamine content was significantly reduced compared with dLRRK WT Tg or control flies (Figure 1D, left). Conversely, dopamine content was elevated in *dLRRK* (−/−) flies, suggesting that dLRRK negatively regulates steady-state dopamine levels (Figure 1D, right). We tested whether this difference in DA content might reflect differential maintenance of DA neurons. In young flies (10-day-old), no difference in DA neuron number was observed when compared with a normal control (Supplementary Figure 3). In aged flies (60-day-old), however, animals expressing pathogenic dLRRK showed a significant reduction of DA neurons in the protocerebral posterior lateral (PPL) 1 and protocerebral posterior medial (PPM) 1 and 2 clusters (Figure 1E). Expression of a kinase-dead form (3KD) of dLRRK or WT dLRRK had no significant effect on DA neuron number (Figure 1E). In both young and aged *dLRRK* (−/−) flies, DA neurons appeared healthy and well maintained (Figure 1E and Supplementary Figure 3). The increase of brain dopamine level in *dLRRK* (−/−) flies is thus likely due to changes of dopamine transmission, storage or metabolism, but not to a change of TH+ neuron number.

Transgenic animals were morphologically normal when dLRRK was ubiquitously expressed. No gross brain degeneration other than DA neuron loss was observed when dLRRK was pan-neuronally expressed, and no neurodegeneration was observed when dLRRK was expressed in specific neuronal types (Supplementary Figure 4 and data not shown), indicating that the toxicity of mutant dLRRK is relatively specific to DA neurons.

Altered dLRRK expression affects organismal sensitivity to oxidative stress

We further analysed animals with altered dLRRK activities to gain insight into the effect of dLRRK on DA neuron maintenance. Oxidative stress is suspected as one of the major causes of DA neuron degeneration in PD. We tested whether dLRRK Tg flies manifest altered response to oxidative stress. Compared with the controls, flies ubiquitously expressing dLRRK Y1383C and I1915T mutants showed significantly higher sensitivity to exogenous ROS inducers paraquat and H_2O_2 (Figure 2A and B). In contrast, *dLRRK* (−/−) or *dLRRK RNAi* animals were significantly more resistant (Figure 2C and D). Animals transheterozygous for *dLRRK* mutant and a chromosomal deficiency that covers *dLRRK* (*Df*/−) were also more resistant to H_2O_2 (Figure 2C and D).

To investigate whether dLRRK is involved in cellular response to endogenous oxidative stress, we examined untreated flies for the extent of oxidative damage as measured

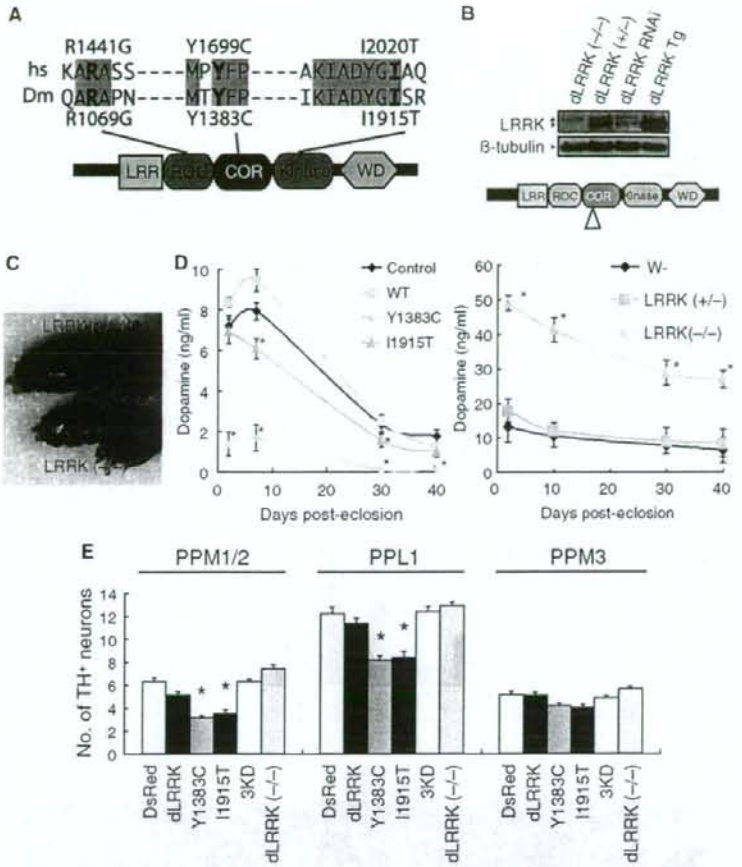

Figure 1 dLRRK regulates function and maintenance of DA neuron. (**A**) A schematic of dLRRK and hLRRK2 domain structures. (**B**) Western blot analysis showing loss of dLRRK protein expression in *dLRRK*(−/−). Brain tissues of 3-day-old adult flies were analysed using anti-dLRRK antibody, which recognizes the N-terminal part of dLRRK. Diagram indicates the location of P-element insertion. (**C**) A phenotype of malformed abdomen observed with incomplete penetrance in *dLRRK*(−/−) females. *dLRRK*(+/−) female shows a normal phenotype. (**D**) Fly heads of dLRRK Tg driven by *Ddc-Gal4* (left) or *dLRRK* mutant animals (right) were used to prepare tissue extracts for dopamine measurement. *Ddc-Gal4*/+ and w^- serves as controls for Tg and *dLRRK* mutant, respectively. The values represent means ± s.e. from five male fly heads in three independent measurements (Asterisk in left and right panels, $P<0.01$ and $P<0.001$, respectively). (**E**) Quantification of TH+ DA neuron number in the PPM 1 and 2, PPL1 and PPM3 clusters in 60-day-old males of the indicated Tg animals driven by *TH-Gal4*. PPM1 and PPM2 cluster neurons were counted together. Data were shown as means ± s.d. (*$P<0.01$ versus *TH-Gal4>DsRed* control, $n=12$ for *dLRRK*(−/−); $n=10$ for the others).

by 4-hydroxy-2-nonenal (4-HNE) immunostaining of lipid peroxidation. An age-dependent increase of 4-HNE level in DA neurons was evident in control flies (Figure 2E and F). In age-matched *dLRRK*(−/−) flies, 4-HNE level was significantly reduced (Figure 2E and F). In contrast, dLRRK Tg animals showed significantly increased 4-HNE levels (Figure 2E and F), with mutant dLRRK showing stronger effect than WT dLRRK. Changes of 4-HNE levels in *dLRRK*(−/−) and Tg animals were confirmed by dot blot analysis of 4-HNE adducts (Supplementary Figure 5A). We also used 2,7-dichlorofluorescein diacetate staining, which is an indicator of hydroxyl-free radical levels, to analyse *dLRRK*(−/−) and Tg flies. Hydroxyl-free radical levels were significantly reduced in *dLRRK* (−/−) and *dLRRK*(*Df*/−) flies, whereas an increase was observed in dLRRK Tg flies (Supplementary Figure 5B). These results suggest a physiological function of dLRRK in handling oxidative stress and a pathological function of heightened oxidative stress in mediating the toxicity of mutant LRRK2.

dLRRK genetically interacts with genes in the TSC/Rheb/TOR/4E-BP pathway

As our previous studies implicated altered PTEN/PI3K/Akt signalling in fly PD models (Yang *et al*, 2005), we tested possible genetic interaction of *dLRRK* with this pathway. *dLRRK* exhibited strong interaction with the TSC/Rheb/TOR/4E-BP pathway, a downstream branch of the PTEN/PI3K/Akt signalling network that regulates cell growth and cell size through protein synthesis. For instance, inhibition of TOR signalling through the co-overexpression of TSC1 and TSC2 inhibited cell growth in the fly eye (Gao and Pan, 2001; Potter *et al*, 2001). This was enhanced by the loss of *dLRRK*

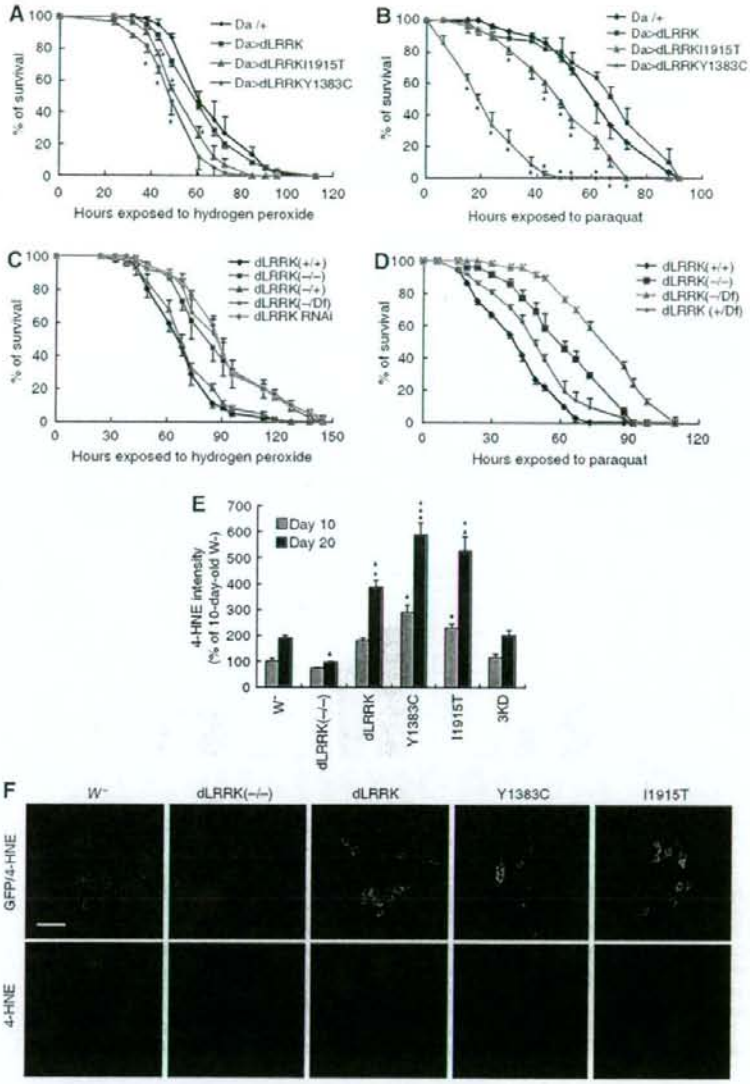

Figure 2 dLRRK regulates stress resistance. **(A)** Response of dLRRK Tg flies to H_2O_2 treatment. Error bars show s.d. from four repeated experiments. $^*P<0.05$, Y1383C and I1915T versus *Da-Gal4/+* control (all, $n=60$). **(B)** Response of dLRRK Tg to paraquat treatment. Error bars show s.d. from three repeated experiments. $^*P<0.05$, Y1383C ($n=48$) and I1915T ($n=48$) versus *Da-Gal4/+* ($n=84$). **(C)** Response of *dLRRK(−/−)* ($n=85$), *dLRRK(Df/−)* ($n=84$) and *dLRRK RNAi* flies ($n=85$) to H_2O_2 treatment. Error bars show s.d. from three repeated experiments. $P<0.01$ versus *dLRRK(+/+)* control ($n=89$) for all values at 61–128 h. *Df/+* and *dLRRK(+/+)* serve as controls. Transgene and RNAi expressions were directed by *Da-Gal4* in A–C. **(D)** Response of *dLRRK(−/−)* ($n=48$) and *dLRRK(Df/−)* flies ($n=46$) to paraquat treatment. Error bars show s.d. from three repeated experiments. $P<0.001$, versus *dLRRK(+/+)* ($n=72$) for all values at 24–73 h. **(E)** Statistical analysis of 4-HNE levels among the indicated genotypes crossed with a *TH-Gal4>UAS-GFP* line at 10- and 20-day of age raised at 29°C. 4-HNE levels from 25–30 TH + neurons in the PPL1 clusters were quantified after normalization with GFP signal. $^*P<0.05$; $^{**}P<0.01$; $^{***}P<0.001$ versus $w^-\times$ *TH-Gal4>GFP* cross (w^-). **(F)** Representative images of PPL1 clusters of the indicated genotypes double-stained for GFP (green) and 4-HNE (red). Scale bar = 20 μm.

(Supplementary Figure 6C), although loss of *dLRRK* in an otherwise WT background had no effect (Supplementary Figure 6A and F). Conversely, stimulation of TOR signalling by Rheb overexpression enhanced cell growth (Saucedo *et al*, 2003), which was partially suppressed by the loss of *dLRRK* (Supplementary Figure 6E and G). Overexpression of a constitutively active form of d4E-BP (4E-BP(LL)), which has stronger affinity for eIF4E (Miron *et al*, 2001), caused a mild reduction of eye size (Supplementary Figure 6H). This effect was significantly enhanced by the loss of *dLRRK* (Supplementary Figure 6I). As the numbers of ommatidia per fly eye and rhabdomeres per ommatidium were not

changed (Supplementary Figure 6J and K), the reduction of eye size was mostly due to a reduction of cell size, a measure of cell growth. The genetic interaction between *dLRRK* and *4E-BP* was also evident in other tissues. Overexpression of 4E-BP(LL) in wing imaginal discs with the *MS1096-Gal4* driver resulted in a moderate reduction of wing size (Miron *et al*, 2001), which was enhanced by the loss of *dLRRK* (Supplementary Figure 6L and N). The effect of removal of *dLRRK* on TSC1, TSC2 and Rheb overexpression was recapitulated by dLRRK knockdown and was rescued by the introduction of dLRRK WT but not 3KD transgenes (Supplementary Figure 7). These results suggest that dLRRK positively regulates cell growth through interaction with the TSC/Rheb/TOR/4E-BP pathway of protein translational control.

LRRK2 phosphorylates 4E-BP

We then sought to investigate the molecular mechanism underlying the effect of dLRRK on protein translation. To study its biochemical function, we purified dLRRK from transfected 293T cells by immunoprecipitation (IP). dLRRK purified this way possessed kinase activity, as shown by autophosphorylation (Figure 3A, upper panel in lane 2 compared with lane 1). As a control, we similarly purified a mutant dLRRK containing three point mutations (3KD), including the K1781 mutation predicted to disrupt ATP-binding (Greggio *et al*, 2006). The 3KD mutant exhibited no kinase activity, suggesting that the activity detected above was derived from dLRRK rather than some associated kinases in the IP complex (Figure 3A, lane 3). We also purified dLRRK containing PD-associated point mutations. The kinase activity of dLRRK containing the I1915T mutation was notably higher than WT dLRRK (Figure 3B, lane 4 compared with lane 2).

Having obtained active dLRRK kinase, we next searched for its substrate(s). On the basis of the genetic interaction data, we tested candidate proteins in the TSC/Rheb/TOR/4E-BP signalling pathway. Robust phosphorylation of d4E-BP by dLRRK was detected (Figure 3A, lane 2). The activities of WT and I1915T mutant dLRRK towards d4E-BP correlated with their autophosphorylation activity (Figure 3B, lanes 2–4). eIF4E, the binding partner of 4E-BP and itself a phospho protein, was not phosphorylated by dLRRK (Supplementary Figure 8), supporting the specificity of dLRRK action towards d4E-BP. The situation holds true for the human proteins, with purified hLRRK2 robustly phosphorylating h4E-BP1 and the I2020T mutant possessing a higher activity (Figure 3C, lane 3 compared with lane 2).

To precisely map the phosphorylation site(s) in h4E-BP1, we made a series of Ser/Thr to Ala substitutions in h4E-BP1 and tested their effects on phosphorylation by hLRRK2 *in vitro*. Mutating T37/T46 and S65 reduced the amount of P^{32} incorporation, whereas mutating T70 and S83 had minimal effect (Figure 3D, lanes 7 and 9 compared with lanes 10 and 12). Combining T37/T46A and S65A mutations further reduced P^{32} incorporation (Figure 3D, lane 3). Addition of a T70A mutation into the T37/T46/S65A triple mutant background had no further effect (Figure 3D, lane 4 compared with lane 3). Western blot analysis of *in vitro*-phosphorylated h4E-BP1 with phospho-specific antibodies showed that the T37/T46 and S65 sites were directly phosphorylated by hLRRK2 (Supplementary Figure 9). Similarly, T37/T46A mutations in *Drosophila* 4E-BP reduced its phosphorylation by dLRRK (Figure 3E, lane 3 compared with lane 2). These *in vitro* results suggest that T37/T46 and S65 in 4E-BP represent major LRRK2 target sites.

To verify the *in vitro* phosphorylation result, we examined the effect of overexpression or knockdown of hLRRK2 on h4E-BP1 phosphorylation. A clear increase of h4E-BP1 phosphorylation at T37/T46 was observed in cells transfected with WT or mutant hLRRK2 (I2020T) (Figure 3F, lanes 2 and 3 compared with lane 1). In contrast, p-T37/T46 level was reduced in cells transfected with hLRRK2 siRNA, which effectively knocked down hLRRK2 expression (Figure 3G), whereas a control siRNA had no effect. As mTOR is known to affect 4E-BP phosphorylation, we tested whether hLRRK2 might exert an effect through mTOR. No change in mTOR phosphorylation or protein level was observed when hLRRK2 activity was altered (Supplementary Figure 10). Thus, the

Figure 3 dLRRK and hLRRK2 phosphorylate 4E-BP. (**A–C**) *In vitro* kinase assays using dLRRK and d4E-BP (A, B) or hLRRK2 and h4E-BP1 (C) as kinase–substrate pairs. Mock immunoprecipitate (IP) serves as control. Autoradiography (P^{32}), western blot (WB) and Coomassie brilliant blue (CBB) staining of the gels are shown. The asterisk in C marks a putative truncated form of hLRRK2 often observed in the IP fraction. (**D, E**) *In vitro* kinase assay using hLRRK2 (D) or dLRRK (E) as the kinase and a series of wild-type (WT) and mutant h4E-BP1 (D) or d4E-BP (E) as substrates. Mock IP serves as kinase control. CBB: protein loading control. The Ser or Thr residues mutated to Ala are indicated. (**F, G**) Western blot analysis showing effects of altered hLRRK2 activities on endogenous h4E-BP1 phosphorylation in 293T cells, which were starved for 24 h and then stimulated with 1 μg/ml insulin for 30 min. (F) Overexpression of WT and I2020T mutant hLRRK2 increased h4E-BP1 phosphorylation at T37/T46 and T70. Mock transfection serves as control. (G) Knockdown of hLRRK2 by RNAi reduced h4E-BP1 phosphorylation at T37/T46 and T70. Control: a non-targeting siRNA. Graphs show relative levels of p-T37/T46, p-T70 and p-S65 after normalization with total h4E-BP1 level. Values represent means ± s.d. from three experiments (*$P<0.05$; **$P<0.01$ in Bonferroni/Dunn test). (**H**) dLRRK influences d4E-BP phosphorylation *in vivo*. d4E-BP protein was immunoprecipitated with a d4E-BP antibody from fly brain extracts of the indicated genotypes. Immunoprecipitated d4E-BP was detected by western blot with p-T37/T46 (upper) and total d4E-BP (lower) antibodies. Bands corresponding to phosphorylated (β) and non-phosphorylated forms (α) of d4E-BP are indicated in the total d4E-BP western. Graph shows relative level of p-T37/T46 after normalization with total d4E-BP level. Values represent means ± s.d. from three experiments (*$P<0.05$; **$P<0.01$ in Bonferroni/Dunn test). (**I, J**) Immunohistochemical analysis showing that dLRRK promotes d4E-BP phosphorylation. Adult brain TH-positive neurons were co-stained with anti-TH and anti-p-T37/T46 in control *w−* or dLRRK Tg crossed with *TH-Gal4*. Representative images are shown in I. The p-T37/T46 signals were quantified after normalization with TH signals. Values represent means ± s.d. from three independent experiments (*$P<0.05$; **$P<0.01$). (**K**) Western blot analysis showing effects of pathogenic hLRRK2 mutations on h4E-BP1 phosphorylation at T37/T46 sites in serum-starved 293T cells. The graph shows quantification of the relative level of p-T37/T46 after normalization with total h4E-BP1 level. Values represent means ± s.d. from three independent experiments (*$P<0.05$; **$P<0.01$ versus hLRRK2 WT). (**L**) hLRRK2 stimulates protein synthesis *in vitro* in a kinase activity-dependent manner. Immunopurified FLAG–hLRRK2 WT, I2020T and 3KD proteins together with capped *firefly* luciferase mRNA were incubated in rabbit reticulocyte lysate (Promega) for 2.5 h at 30 °C. The activity of luciferase translated in the lysate was measured (graph, means ± s.d. from three independent experiments). *$P<0.05$ versus mock. Western blot and RT–PCR was performed for estimation of protein and mRNA levels in the lysate. PCR without RT (PCR) serves as a negative control for RT–PCR.

T37/T46 sites in h4E-BP1 appeared to be physiological hLRRK2 target sites. Despite the fact that T70 was not directly modified by hLRRK2 *in vitro*, its phosphorylation was affected by alterations of hLRRK2 in the cultured cells (Figure 3F and G). This is consistent with the notion that p-T37/T46 may prime subsequent T70 phosphorylation (Gingras *et al*, 2001) by other kinases. Alternatively, T70 could be a direct target of dLRRK *in vivo*. On the other hand, although S65 was modified by hLRRK2 *in vitro*, its phosphorylation was not affected by hLRRK2 in cultured cells (Figures 3F and G). The S65 site may be more tightly regulated by other kinases or phosphatases *in vivo*.

We sought for further *in vivo* evidence that LRRK2 is a 4E-BP kinase. Western blot and immunostaining of dLRRK Tg and mutant flies showed that phosphorylation of d4E-BP at T37/T46 sites was increased in dLRRK Tg but decreased in *dLRRK*(−/−) flies, supporting the fact that T37/T46 in d4E-BP are *in vivo* dLRRK target sites (Figure 3H–J). Note that, in *dLRRK*(−/−) mutant flies, phosphorylation of d4E-BP at T37/T46 sites was reduced but not abolished, suggesting that there exist other kinase(s) that exert an effect on these sites. Both WT and a pathogenic LRRK2 effectively stimulated the phosphorylation of T37/T46 sites of 4E-BP1 to similar levels upon insulin treatment (Figure 3F). Under starvation (serum-free) condition, however, some pathogenic mutants exhibit higher kinase activity than WT LRRK2 (Figure 3K). These data suggested that LRRK2 interacts with the insulin/IGF signalling pathway to regulate 4E-BP phosphorylation, but

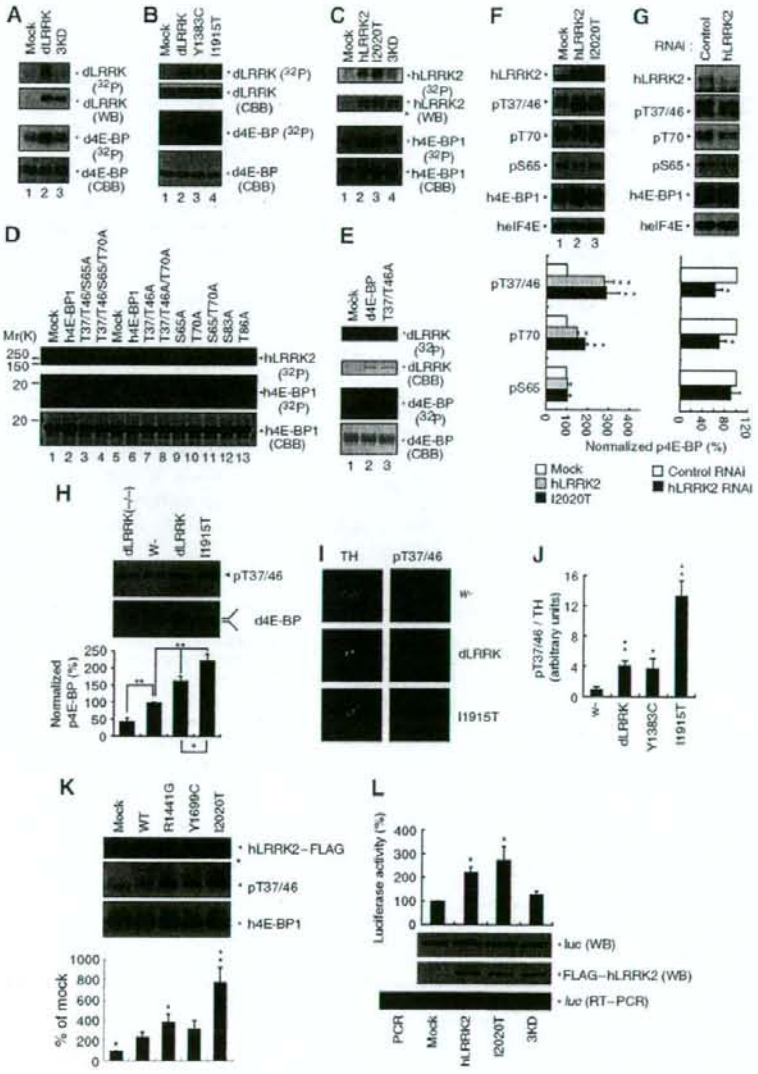

the kinase activity of some pathogenic mutants is not dependent on insulin/IGF stimulation.

The genetic interaction between *LRRK2* and the TSC/Rheb/TOR/4E-BP pathway of growth control and the phosphorylation of 4E-BP by LRRK2 suggest that LRRK2 is a positive regulator of protein translation. Consistent with this notion, direct addition of purified hLRRK2 WT and I2020T proteins to an *in vitro* translation system effectively stimulated the translation of a luciferase reporter mRNA, whereas hLRRK2 3KD had no effect (Figure 3L).

Activities of 4E-BP and eIF4E are important for cellular stress response and DA neuron maintenance

Previous studies revealed a function for d4E-BP in conferring resistance against starvation and oxidative stress (Teleman *et al*, 2005; Tettweiler *et al*, 2005). We asked whether phosphorylation of 4E-BP at T37/T46 residues, which is promoted by dLRRK kinase activity, affects resistance to oxidative stress *in vivo*. For this purpose, we generated Tg flies expressing d4E-BP T37/T46A (TA) mutant protein. Whereas expression of d4E-BP WT restored oxidative stress resistance in *d4E-BP*(−/−), expression of similar levels of d4E-BP TA resulted in higher resistance against oxidative stress (Figure 4A and B, and Supplementary Figure 11). This suggests that complete blockage of 4E-BP T37/T46 phosphorylation and the consequent tighter binding and stronger inhibition of eIF4E lead to higher stress resistance. To test this idea further, we asked whether manipulation of eIF4E is sufficient to alter oxidative stress response. Overexpression of delF4E significantly sensitized animals to oxidative stress treatments, similar to the effect induced by mutant dLRRK overexpression (Figure 4C). Furthermore, delF4E Tg animals showed a significant increase of 4-HNE in the absence of stress (Figure 4D), suggesting that excessive eIF4E activity altered endogenous stress response and resulted in more oxidative damages.

Consistent with the above findings, removal of one copy of *delF4E* in dLRRK I1915T Tg flies increased resistance against oxidative stress (Figure 4E). We further tested whether the co-expression of d4E-BP TA mutant, by inhibiting the release of d4E-BP from delF4E, rendered dLRRK I1915T flies more resistant to oxidative stress. This was indeed the case (Supplementary Figure 12). We next used 7-methyl GTP (m^7GTP) sepharose-binding assay to biochemically assess the level of 4E-BP-free eIF4E, an indicator of translation efficiency, in the various genetic backgrounds. *In vivo*, eIF4E protein level is fairly constant and both the 4E-BP-bound and 4E-BP-free forms of eIF4E bind to m^7GTP sepharose beads. By measuring the amount of 4E-BP-bound eIF4E, we can get an estimate of 4E-BP-free, active eIF4E. As shown in Figure 4F, in d4E-BP WT Tg animals co-expressing GFP, a significant portion of d4E-BP WT was released from delF4E under normal conditions; however, under oxidative stress condition, almost all d4E-BP WT was bound to delF4E (Figure 4F, lanes 1 and 2). The amount of d4E-BP WT released from delF4E was increased in the presence of dLRRK I1915T under both normal and oxidative stress conditions (Figure 4F, lanes 3 and 4). In contrast, d4E-BP TA was tightly bound to eIF4E in the presence or absence of dLRRK I1915T, and under normal or stress conditions (Figure 4F, lanes 5–8). These results suggested that dLRRK releases the inhibition of eIF4E by 4E-BP, enabling free eIF4E to engage in translation.

We next tested whether d4E-BP and delF4E influence dLRRK-mediated DA neurodegeneration in the flies. Whereas overexpression of d4E-BP had no effect on DA neuron number in control Tg flies, it partially suppressed the DA neuron loss phenotype seen in dLRRK Tg flies (Figure 5A). Introduction of d4E-BP TA fully protected against DA neuron loss caused by dLRRK I1915T (Figure 5B). Furthermore, introduction of d4E-BP WT rescued DA neuron loss seen in *d4E-BP*(−/−) flies (Figure 5B). Supporting a function for deregulation of the eIF4E/4E-BP pathway in inducing DA neuron loss, overexpression of delF4E alone caused a reduction of DA neurons; however, in *dLRRK*(−/−) background, this effect of delF4E was suppressed (Figure 5C). Given that DA neuron loss was observed in aged dLRRK Tg flies, we searched for evidence of motor dysfunction caused by DA degeneration. As shown in Figure 5D, dLRRK I1915T expression caused locomotor dysfunction with age, which was improved by the co-expression of d4E-BP TA (Figure 5D). Taken together, these results indicate that the interaction between dLRRK and the eIF4E/4E-BP pathway is intimately involved in the maintenance of DA neurons.

Discussion

In this study, we used *Drosophila* as a model system to understand the normal physiological function of LRRK2 and how its dysfunction leads to DA neurodegeneration. We provide genetic and biochemical evidence that dLRRK modulates the maintenance of DA neuron by regulating protein synthesis. We demonstrate that LRRK2 primes phosphorylation of 4E-BP and that this event has an important function in mediating the pathogenic effects of mutant dLRRK. These results for the first time link deregulation of the eIF4E/4E-BP pathway of protein translation with DA degeneration in PD.

eIF4E is a key component of the eIF4F complex that initiates cap-dependent protein synthesis. It has long been recognized that a key mechanism regulating eIF4E function is through phosphorylation-induced release of 4E-BP from eIF4E. A number of candidate kinases, including mTOR, have been implicated on the basis of *in vitro* or cell culture studies, but the physiological kinases remain to be identified. We show here that LRRK2 is one of the physiological kinases for 4E-BP. LRRK2 exerts an effect on 4E-BP primarily at the T37/T46 sites. Phosphorylation at T37/T46 by LRRK2 likely facilitates subsequent phosphorylation at T70 and S65 *in vivo* by other kinase or LRRK2 itself. 4E-BP phosphorylation by LRRK2, therefore, could serve as an initiating event in an ordered, multisite phosphorylation process to generate hyperphosphorylated 4E-BP (Figure 6), similar to the phosphorylation of the Alzheimer's disease-associated tau (Nishimura *et al*, 2004). Our results show that LRRK2 is not the only kinase that phosphorylates 4E-BP T37/T46 sites (Figure 3H). Similarly, 4E-BP is unlikely the only substrate of LRRK2. A recent study showed that human LRRK2 phosphorylates moesin (Jaleel *et al*, 2007), the physiological relevance of which remains to be determined.

The role of 4E-BP in regulating eIF4E function has been well established *in vitro*. Recent studies in *Drosophila*, however, have revealed the complexity of the *in vivo* function of 4E-BP. Loss of the only *d4E-BP* gene does not affect cell size

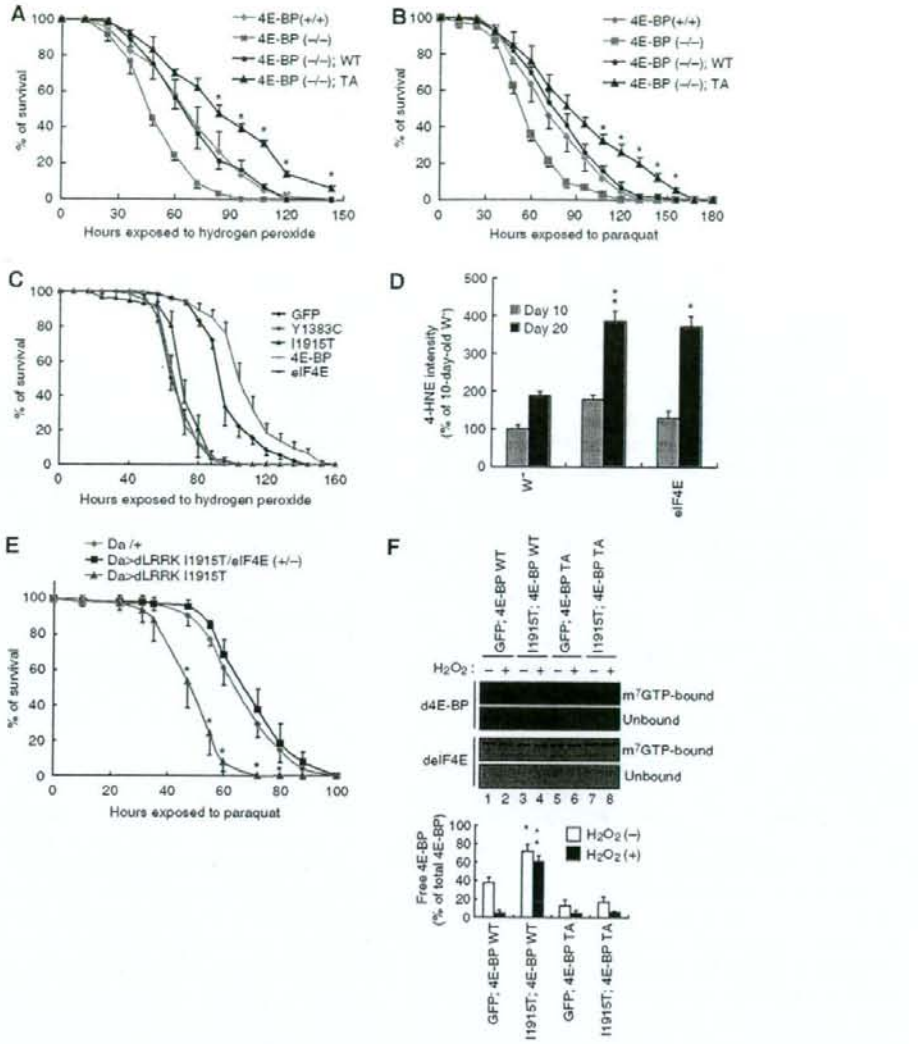

Figure 4 The eIF4E/4E-BP pathway is important for handling oxidative stress. (**A**, **B**) d4E-BP TA confers H_2O_2 (A) and paraquat (B) resistance. d4E-BP WT or TA mutant were expressed in the *d4E-BP(−/−)* background under *DA-Gal4* control. *$P<0.05$, *d4E-BP(−/−); TA* ($n=76$ in A; $n=78$ in B) versus *d4E-BP(−/−); WT* ($n=80$ in A; $n=82$ in B). (**C**) Oxidative stress responses of dLRRK, delF4E and d4E-BP Tg flies driven by *Da-Gal4*. delF4E Tg ($n=72$) and the dLRRK Y1383C ($n=72$) or I1915T ($n=85$) Tg were more sensitive to H_2O_2 treatment than the GFP Tg control ($n=90$) ($P<0.01$ for all values at 72–120 h), whereas d4E-BP Tg ($n=90$) was more resistant than the control ($P<0.05$ versus GFP Tg for the values at 72–144 h). (**D**) Overexpression of delF4E or dLRRK increases 4-HNE levels in DA neurons. *TH-Gal4>GFP* was crossed with the indicated genotypes as shown in Figure 2E. Values represent means ± s.d. (*$P<0.05$; **$P<0.01$ versus age-matched *w−*, $n=25$–30). Error bars in (A–D) show s.d. from three repeated experiments. (**E**) Reduction of delF4E function suppresses vulnerability of dLRRK I1915T to oxidative stress induced by paraquat. dLRRK I1915T was expressed in the *delF4E(+/+)* or *delF4E(+/−)* background with *DA-Gal4*. *$P<0.006$, *Da>dLRRK I1915T/delF4E* (+/−) ($n=74$) versus *Da>dLRRK I1915T* ($n=75$). (**F**) m^7GTP pull-down assay showing the effect of dLRRK I1915T on free eIF4E levels. eIF4E was precipitated using m^7GTP-sepharose from the brain tissues of flies with or without 5% H_2O_2 treatment for 24 h. eIF4E-bound (m^7GTP-bound) and free (unbound) 4E-BP were estimated. Graph shows the percentage of free 4E-BP in total 4E-BP after normalization with m^7GTP-bound eIF4E level. Values represent means ± s.d. from three experiments (*$P<0.05$; **$P<0.01$ versus GFP; 4E-BP WT in corresponding treatment).

or animal viability (Bernal and Kimbrell, 2000), suggesting that it is dispensable for cell growth or survival under normal conditions. However, *d4E-BP* mutant flies are defective in responses to various stress stimuli (Bernal and Kimbrell, 2000; Teleman *et al*, 2005; Tettweiler *et al*, 2005). d4E-BP has also been proposed to exert an effect as a metabolic brake for fat metabolism under stress conditions (Teleman *et al*, 2005). Whether this role of 4E-BP is relevant to dLRRK function in stress resistance and DA neuron maintenance remains to be tested. eIF4E, the target of 4E-BP, functions

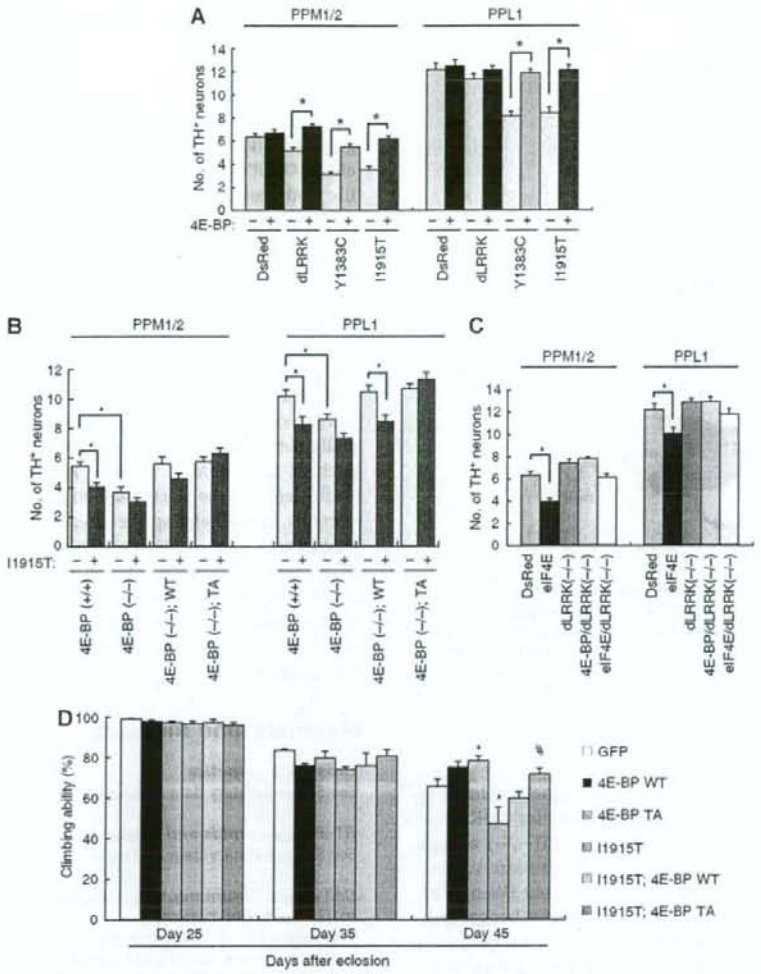

Figure 5 4E-BP overexpression suppresses dysfunction and degeneration of DA neuron induced by mutant dLRRK. (**A**) d4E-BP co-expression rescues dLRRK overexpression-induced DA neuron loss (*$P<0.01$ in Student's *t*-test, $n=12$). *TH-Gal4* was used to direct transgene expression and 60-day-old flies aged at 25 °C were analysed. (**B**) d4E-BP TA protects against DA neuron loss in dLRRK I1915T Tg flies. *TH-Gal4* was used to direct transgene expression and 30-day-old flies aged at 29 °C were analysed. *$P<0.05$, $n=14$. (**C**) *dLRRK* LOF rescues deIF4E overexpression-induced DA neuron loss (*$P<0.01$, $n=12$). *TH-Gal4* crosses were analysed as in (**A**). (**D**) Pan-neuronal expression of dLRRK I1915T under *elav-Gal4* control leads to gradual motor defect with age. The loss of climbing ability in dLRRK I1915T-expressing flies was rescued by 4E-BP TA expression. GFP serves as control. The values represent means ± s.d. from 20 trials ($n=30$; *$P<0.05$ versus GFP; #$P<0.01$ versus I1915T by one-way ANOVA with Bonferroni/Dunn test). The genotypes are as follows: *elav-Gal4>UAS-GFP* (GFP), *elav-Gal4>UAS-4E-BP WT* (4E-BP WT), *elav-Gal4>UAS-4E-BP TA* (4E-BP TA), *elav-Gal4>UAS-dLRRK I1915T* (I1915T), *elav-Gal4>UAS-dLRRK I1915T/UAS-4E-BP WT* (I1915T; 4E-BP WT), *elav-Gal4>UAS-dLRRK I1915T/UAS-4E-BP TA* (I1915T; 4E-BP TA). Male flies were used for the assay.

primarily in regulating general protein translation *in vitro*. It has been suggested that overactivation of eIF4E is linked to the aging process and lifespan regulation *in vivo* (Ruggero *et al*, 2004; Syntichaki *et al*, 2007). We observed that overexpression of eIF4E as well as dLRRK leads to an aging-related phenotype in DA neurons, which strongly suggested that chronic attenuation of 4E-BP activity promotes oxidative stress and consequent aging in DA neurons. This is consistent with the finding of similar patterns of gene expression under oxidative stress and aging conditions (Landis *et al*, 2004), and the fact that PD caused by LRRK2 mutations is of late onset, with aging being a major risk factor.

We analysed effects of removing dLRRK activity using a transposon insertion allele (*dLRRK−*), a chromosomal deletion allele (*dLRRK Df*) and gene knockdown (*dLRRK* RNAi). *dLRRK(−/−)*, *dLRRK* (*Df/−*) and *dLRRK* RNAi flies are all resistant to oxidative stress treatments and show reduced endogenous ROS damages. In the paraquat treatment assay, *dLRRK* (*Df/−*) appeared more resistant than *dLRRK(−/−)* (Figure 2D). It is possible that *dLRRK(−/−)*, which contains a transposon insertion in the COR domain of dLRRK, is not a null allele, although we have not been able to detect a truncated protein product using an antibody against the N-terminus of the protein. Alternatively, the chromosomal

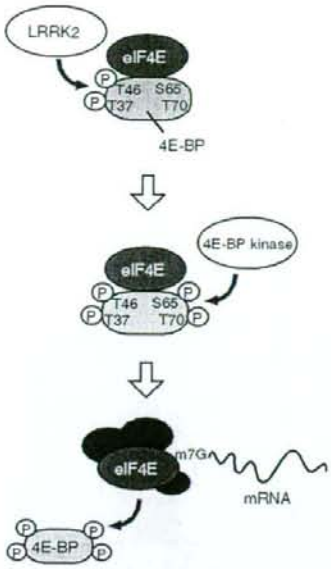

Figure 6 A model depicting 4E-BP phosphorylation by dLRRK. Phosphorylation of 4E-BP at T37/T46 residues by LRRK2 (upper) facilitates subsequent phosphorylation at T70 and S65 (middle). Hyperphosphorylated 4E-BP is released from mRNA cap-binding protein eIF4E, which leads to the formation of an initiation factor complex including eIF4E for protein translation (lower).

deletion in *dLRRK* (*Df*) may include other gene(s) relevant to stress sensitivity. One candidate is the gene for PI3K *Dp110* subunit. A recent study reported that *dLRRK*(−/−) animals are slightly sensitive to hydrogen peroxide but are comparable to control animals in response to paraquat (Wang *et al*, 2008). It is possible that the different genetic backgrounds and the nutrient conditions may account for the divergent results. In our studies, we backcrossed the mutant chromosome to w^- WT background for six generations in an effort to eliminate potential background mutations. A consistent finding from our study and two other studies of *dLRRK*(−/−) animals is that dLRRK is dispensable for the maintenance of DA neurons (Lee *et al*, 2007; Wang *et al*, 2008), although in one study it was reported that *dLRRK*(−/−) animals show reduced TH immunoreactivity and shrunken morphology of DA neurons (Lee *et al*, 2007). In contrast, overexpression of hLRRK2 containing a pathogenic G2019S mutation (Liu *et al*, 2008), or overexpression of mutant dLRRK as reported here, caused DA neuron degeneration, supporting the fact that the pathogenic mutations cause disease by a GOF mechanism.

The pathogenesis caused by mutations in LRRK2 could be partially explained by their higher kinase activity. Indeed, some pathogenic mutants of both hLRRK2 and dLRRK show elevated kinase activity towards 4E-BP. However, other mutants (e.g., hLRRK2 Y1699C and dLRRK Y1383C) did not show elevated kinase activity *in vivo*. Therefore, these pathogenic hLRRK2 mutations might confer cellular toxicity through mechanisms other than protein translation. For example, some hLRRK2 mutants are prone to aggregation in cultured cells (Smith *et al*, 2005; Greggio *et al*, 2006). Consistently, dLRRK Y1383C mutant appeared as more prominent vesicular aggregates in fly DA neurons (data not shown). Nevertheless, the facts that overexpression of eIF4E is sufficient to confer hypersensitivity to oxidative stress and DA neuron loss and that co-expression of 4E-BP suppresses the dopaminergic toxicity caused by more than one pathogenic dLRRK mutants provide compelling evidence that the eIF4E–4E-BP axis has an important function in mediating the pathogenic effects of overactivated LRRK2. The more downstream events that lead to DA neurotoxicity remain to be elucidated. So far, we have found no clear evidence of altered autophagy, caspase activation or DNA fragmentation (data not shown).

There are several possibilities of how elevated protein translation could contribute to PD pathogenesis. First, given that protein synthesis is a highly energy-demanding process, stimulation of protein translation by LRRK2 could perturb cellular energy and redox homoeostasis. This could be especially detrimental in aged cells or stressed post-mitotic cells such as DA neurons. Second, increased protein synthesis could lead to the accumulation of misfolded or aberrant proteins, overwhelming the already compromised ubiquitin proteasome and molecular chaperone systems in aged or stressed cells. Third, altered LRRK2 kinase activity may affect synapse structure and function, which is known to involve local protein synthesis. Deregulation of this process could lead to synaptic dysfunction and eventual neurodegeneration.

Materials and methods

Drosophila genetics

See Supplementary data for details.

RT–PCR, plasmids and siRNAs

See Supplementary data for details.

Cell culture, immunopurification, western blot analysis and m^7GTP pull-down assay

Transfection of 293T cell, immunopurification of FLAG-protein from the transfected cell lysate and western blot analysis were performed as described previously (Imai *et al*, 2000, 2001). For preparation of fly samples for western blot analysis, fly heads were directly homogenized in 20 μl of SDS sample buffer per head using a motor-driven pestle. After centrifugation at 16 000*g* for 10 min, the supernatant was used in SDS–PAGE. For immunoprecipitation or m^7GTP pull-down assay, fly heads were homogenized in 10 μl of lysis buffer per head (50 mM Tris, pH 7.4, 150 mM NaCl, 5 mM EDTA, 10% glycerol, 1% Triton X-100, 0.5 mM DTT, 60 mM β-glycerolphosphate, 1 mM sodium vanadate, 20 mM NaF and complete inhibitor cocktail (Roche)). After centrifugation at 16 000*g* for 30 min, the supernatant was subjected to the assays. For m^7GTP pull-down assay, the supernatant of each lysate from 15 fly heads was incubated with 15 μl of m^7GTP-Sepharose (GE Healthcare) for 2 h. The precipitates were washed four times with lysis buffer. The precipitates (m^7GTP-bound) and the flow through (unbound) were analysed by western blot. Densitometry was analysed using Image J software from the US National Institute of Health (http//rsb.info.nih.gov/ij/).

Antibodies

See Supplementary data for details of antibodies resources.

In vitro phosphorylation assay

FLAG–dLRRK or FLAG–hLRRK2 immunopurified from transfected 293T cells and mock fractions processed by the same procedures were used as kinase sources. Five micrograms of His–d4E-BP or His–h4E-BP1 were incubated with FLAG–dLRRK or FLAG–hLRRK2 in a kinase reaction buffer (20 mM HEPES, pH 7.4, 15 mM $MgCl_2$, 5 mM EGTA, 0.1% Triton X-100, 0.5 mM DTT, 1 mM β-glycerolpho-

sphate and 2.5 μCi [γ-^{32}P]-ATP) for 30 min at 30 °C. The reaction mixture was suspended in SDS sample buffer and then subjected to SDS–PAGE and autoradiography.

Dopamine measurement

Monoamine measurement was performed as described previously (Yang *et al*, 2005), with investigators blind to the genotypes during the measurement.

Whole-mount immunostaining

Counting of TH-positive neurons was performed by whole-mount immunostaining of brain samples as described previously (Yang *et al*, 2006). Immunohistochemical analysis for 4-HNE was carried out in whole-mount brain samples of animals originated from *TH-Gal4>UAS-GFP* crossed to the indicated genotypes. Anti-4HNE signals were normalized with GFP signals derived from the UAS-GFP transgene expressed in the same TH-positive neurons. Image J software was used for signal quantification. For dot blot analysis of 4-HNE, total lysates made from fly heads were spotted onto a PVDF membrane and subsequently incubated with anti-4HNE (1:15) overnight. As a control, we used western blot analysis of β-tubulin from the same extracts. Properties of the 4-HHE antibody are described on the manufacturer's Web site: http://www.jaica.com/biotech/e/. Immunohistochemical analyses were performed using a Carl Zeiss laser scanning microscope system.

Oxidative stress assay

The survival rate of 10-day-old male adult flies ($n=15$–20 per vial) kept in a vial containing a tissue paper socked with 0.5% H_2O_2 or 2 mM paraquat prepared in Schneider's insect medium was measured as described (Yang *et al*, 2005). To control for isogeny, *dLRRK(−/−)*, *4E-BP(−/−)*, *UAS-4E-BP* and the *Da-Gal4* driver were backcrossed to w^- background for six generations. For studies in transgenic overexpression, the *UAS-dLRRK* transgenes, *UAS-dLRRK RNAi* and *UAS-d4E-BP TA* transgenic lines were generated in w^- background and thus have a matched genetic background. For the analysis in Figures 4 and 5, *Thor*^{1} (*4E-BP null*) and its revertant served as 4E-BP(−/−) and 4E-BP(+/+), respectively. *UAS-d4E-BP WT* and *UAS-d4E-BP TA* transgenics, which shows similar protein expression of d4E-BP, were backcrossed to 4E-BP(−/−) background for five generations.

Climbing assay

The climbing assay was performed similarly to a previously described protocol (Feany and Bender, 2000). Thirty flies were placed in a plastic vial (18.6 cm in height × 3.5 cm^2 in area) and gently tapped to bring them down to the bottom of the vial. Flies were given 18 s to climb, and the number of flies above 6 cm from the bottom was counted. Twenty trials were performed for each time point for the same set of flies.

Statistical analysis

Two-way repeated-measures ANOVA was performed in multiple groups unless otherwise indicated. If positive ($P<0.05$), the means between the control and the specific groups were analysed using the Dunnett's test.

Supplementary data

Supplementary data are available at *The EMBO Journal* Online (http://www.embojournal.org).

Acknowledgements

We are grateful to Drs B Edgar, DA Kimbrell, P Lasko, D Pan, N Sonenberg, Z Zhang, T Xu and the *Drosophila* Stock centers for flies; Drs NJ Dyson, P Lasko, N Sonenberg and J Sierra, and RH Wharton for antibodies; Drs P Bitterman and V Polunovsky for plasmids; and Dr S Guo for reading the manuscripts. Special thanks go to J Quach, Y Zhang and W Lee for technical supports and members of the Lu lab for discussions. Supported by the NIH (R21 NS056878-01, R01 AR054926-01), the McKnight, Beckman and Sloan Foundations (BL), the Naito Foundation, JSPS Postdoctoral Fellowships for Research Abroad and Program for Young Researchers from Special Coordination Funds for Promoting Science and Technology commissioned by MEXT in Japan (YI).

References

Bernal A, Kimbrell DA (2000) *Drosophila* Thor participates in host immune defense and connects a translational regulator with innate immunity. *Proc Natl Acad Sci USA* **97:** 6019–6024

Fadden P, Haystead TA, Lawrence Jr JC (1997) Identification of phosphorylation sites in the translational regulator, PHAS-I, that are controlled by insulin and rapamycin in rat adipocytes. *J Biol Chem* **272:** 10240–10247

Feany MB, Bender WW (2000) A *Drosophila* model of Parkinson's disease. *Nature* **404:** 394–398

Gao X, Pan D (2001) TSC1 and TSC2 tumor suppressors antagonize insulin signaling in cell growth. *Genes Dev* **15:** 1383–1392

Gingras AC, Gygi SP, Raught B, Polakiewicz RD, Abraham RT, Hoekstra MF, Aebersold R, Sonenberg N (1999a) Regulation of 4E-BP1 phosphorylation: a novel two-step mechanism. *Genes Dev* **13:** 1422–1437

Gingras AC, Raught B, Gygi SP, Niedzwiecka A, Miron M, Burley SK, Polakiewicz RD, Wyslouch-Cieszynska A, Aebersold R, Sonenberg N (2001) Hierarchical phosphorylation of the translation inhibitor 4E-BP1. *Genes Dev* **15:** 2852–2864

Gingras AC, Raught B, Sonenberg N (1999b) eIF4 initiation factors: effectors of mRNA recruitment to ribosomes and regulators of translation. *Annu Rev Biochem* **68:** 913–963

Gloeckner CJ, Kinkl N, Schumacher A, Braun RJ, O'Neill E, Meitinger T, Kolch W, Prokisch H, Ueffing M (2006) The Parkinson disease causing LRRK2 mutation I2020T is associated with increased kinase activity. *Hum Mol Genet* **15:** 223–232

Greggio E, Jain S, Kingsbury A, Bandopadhyay R, Lewis P, Kaganovich A, van der Brug MP, Beilina A, Blackinton J, Thomas KJ, Ahmad R, Miller DW, Kesavapany S, Singleton A, Lees A, Harvey RJ, Harvey K, Cookson MR (2006) Kinase activity is required for the toxic effects of mutant LRRK2/dardarin. *Neurobiol Dis* **23:** 329–341

Heesom KJ, Avison MB, Diggle TA, Denton RM (1998) Insulin-stimulated kinase from rat fat cells that phosphorylates initiation factor 4E-binding protein 1 on the rapamycin-insensitive site (serine-111). *Biochem J* **336** (Part 1): 39–48

Holcik M, Sonenberg N (2005) Translational control in stress and apoptosis. *Nat Rev Mol Cell Biol* **6:** 318–327

Imai Y, Soda M, Inoue H, Hattori N, Mizuno Y, Takahashi R (2001) An unfolded putative transmembrane polypeptide, which can lead to endoplasmic reticulum stress, is a substrate of Parkin. *Cell* **105:** 891–902

Imai Y, Soda M, Takahashi R (2000) Parkin suppresses unfolded protein stress-induced cell death through its E3 ubiquitin-protein ligase activity. *J Biol Chem* **275:** 35661–35664

Inoki K, Corradetti MN, Guan KL (2005) Dysregulation of the TSC-mTOR pathway in human disease. *Nat Genet* **37:** 19–24

Jaleel M, Nichols RJ, Deak M, Campbell DG, Gillardon F, Knebel A, Alessi DR (2007) LRRK2 phosphorylates moesin at threonine-558: characterization of how Parkinson's disease mutants affect kinase activity. *Biochem J* **405:** 307–317

Jenner P (2003) Oxidative stress in Parkinson's disease. *Ann Neurol* **53** (Suppl 3): S26–S36; discussion S28–S36

Landis GN, Abdueva D, Skvortsov D, Yang J, Rabin BE, Carrick J, Tavare S, Tower J (2004) Similar gene expression patterns characterize aging and oxidative stress in Drosophila melanogaster. *Proc Natl Acad Sci USA* **101:** 7663–7668

Lee SB, Kim W, Lee S, Chung J (2007) Loss of LRRK2/PARK8 induces degeneration of dopaminergic neurons in *Drosophila*. *Biochem Biophys Res Commun* **358:** 534–539

Liu Z, Wang X, Yu Y, Li X, Wang T, Jiang H, Ren Q, Jiao Y, Sawa A, Moran T, Ross CA, Montell C, Smith WW (2008) A *Drosophila* model for LRRK2-linked parkinsonism. *Proc Natl Acad Sci USA* **105:** 2693–2698

Mata IF, Wedemeyer WJ, Farrer MJ, Taylor JP, Gallo KA (2006) LRRK2 in Parkinson's disease: protein domains and functional insights. *Trends Neurosci* **29:** 286–293

Miron M, Verdu J, Lachance PE, Birnbaum MJ, Lasko PF, Sonenberg N (2001) The translational inhibitor 4E-BP is an effector of PI(3)K/Akt signalling and cell growth in *Drosophila*. *Nat Cell Biol* **3:** 596–601

Moore DJ, West AB, Dawson VL, Dawson TM (2005) Molecular pathophysiology of Parkinson's disease. *Annu Rev Neurosci* **28:** 57–87

Nishimura I, Yang Y, Lu B (2004) PAR-1 kinase plays an initiator role in a temporally ordered phosphorylation process that confers tau toxicity in *Drosophila*. *Cell* **116:** 671–682

Paisan-Ruiz C, Jain S, Evans EW, Gilks WP, Simon J, van der Brug M, Lopez de Munain A, Aparicio S, Gil AM, Khan N, Johnson J, Martinez JR, Nicholl D, Carrera IM, Pena AS, de Silva R, Lees A, Marti-Masso JF, Perez-Tur J, Wood NW *et al* (2004) Cloning of the gene containing mutations that cause PARK8-linked Parkinson's disease. *Neuron* **44:** 595–600

Potter CJ, Huang H, Xu T (2001) *Drosophila* Tsc1 functions with Tsc2 to antagonize insulin signaling in regulating cell growth, cell proliferation, and organ size. *Cell* **105:** 357–368

Richter JD, Sonenberg N (2005) Regulation of cap-dependent translation by eIF4E inhibitory proteins. *Nature* **433:** 477–480

Ruggero D, Montanaro L, Ma L, Xu W, Londei P, Cordon-Cardo C, Pandolfi PP (2004) The translation factor eIF-4E promotes tumor formation and cooperates with c-Myc in lymphomagenesis. *Nat Med* **10:** 484–486

Saucedo LJ, Gao X, Chiarelli DA, Li L, Pan D, Edgar BA (2003) Rheb promotes cell growth as a component of the insulin/TOR signalling network. *Nat Cell Biol* **5:** 566–571

Smith WW, Pei Z, Jiang H, Moore DJ, Liang Y, West AB, Dawson VL, Dawson TM, Ross CA (2005) Leucine-rich repeat kinase 2 (LRRK2) interacts with parkin, and mutant LRRK2 induces neuronal degeneration. *Proc Natl Acad Sci USA* **102:** 18676–18681

Sonenberg N, Rupprecht KM, Hecht SM, Shatkin AJ (1979) Eukaryotic mRNA cap binding protein: purification by affinity chromatography on sepharose-coupled m^7GDP. *Proc Natl Acad Sci USA* **76:** 4345–4349

Syntichaki P, Troulinaki K, Tavernarakis N (2007) eIF4E function in somatic cells modulates ageing in *Caenorhabditis elegans*. *Nature* **445:** 922–926

Taylor JP, Mata IF, Farrer MJ (2006) LRRK2: a common pathway for parkinsonism, pathogenesis and prevention? *Trends Mol Med* **12:** 76–82

Teleman AA, Chen YW, Cohen SM (2005) 4E-BP functions as a metabolic brake used under stress conditions but not during normal growth. *Genes Dev* **19:** 1844–1848

Tettweiler G, Miron M, Jenkins M, Sonenberg N, Lasko PF (2005) Starvation and oxidative stress resistance in *Drosophila* are mediated through the eIF4E-binding protein, d4E-BP. *Genes Dev* **19:** 1840–1843

Wang D, Tang B, Zhao G, Pan Q, Xia K, Bodmer R, Zhang Z (2008) Dispensable role of *Drosophila* ortholog of LRRK2 kinase activity in survival of dopaminergic neurons. *Mol Neurodegener* **3:** 3

West AB, Moore DJ, Biskup S, Bugayenko A, Smith WW, Ross CA, Dawson VL, Dawson TM (2005) Parkinson's disease-associated mutations in leucine-rich repeat kinase 2 augment kinase activity. *Proc Natl Acad Sci USA* **102:** 16842–16847

Yamaguchi S, Ishihara H, Yamada T, Tamura A, Usui M, Tominaga R, Munakata Y, Satake C, Katagiri H, Tashiro F, Aburatani H, Tsukiyama-Kohara K, Miyazaki J, Sonenberg N, Oka Y (2008) ATF4-mediated induction of 4E-BP1 contributes to pancreatic beta cell survival under endoplasmic reticulum stress. *Cell Metab* **7:** 269–276

Yang Y, Gehrke S, Haque ME, Imai Y, Kosek J, Yang L, Beal MF, Nishimura I, Wakamatsu K, Ito S, Takahashi R, Lu B (2005) Inactivation of *Drosophila* DJ-1 leads to impairments of oxidative stress response and phosphatidylinositol 3-kinase/Akt signaling. *Proc Natl Acad Sci USA* **102:** 13670–13675

Yang Y, Gehrke S, Imai Y, Huang Z, Ouyang Y, Wang JW, Yang L, Beal MF, Vogel H, Lu B (2006) Mitochondrial pathology and muscle and dopaminergic neuron degeneration caused by inactivation of *Drosophila* Pink1 is rescued by Parkin. *Proc Natl Acad Sci USA* **103:** 10793–10798

Zimprich A, Biskup S, Leitner P, Lichtner P, Farrer M, Lincoln S, Kachergus J, Hulihan M, Uitti RJ, Calne DB, Stoessl AJ, Pfeiffer RF, Patenge N, Carbajal IC, Vieregge P, Asmus F, Muller-Myhsok B, Dickson DW, Meitinger T, Strom TM *et al* (2004) Mutations in LRRK2 cause autosomal-dominant parkinsonism with pleomorphic pathology. *Neuron* **44:** 601–607

Journal of Neurochemistry

JNC

JOURNAL OF NEUROCHEMISTRY | 2008 | 107 | 171–185

doi: 10.1111/j.1471-4159.2008.05607.x

Pael-R transgenic mice crossed with parkin deficient mice displayed progressive and selective catecholaminergic neuronal loss

Hua-Qin Wang,*,†,‡ Yuzuru Imai,§ Haruhisa Inoue,*,†,¶ Ayane Kataoka,† Sachiko Iita,† Nobuyuki Nukina† and Ryosuke Takahashi*,†,¶

*Department of Neurology, Kyoto University Graduate School of Medicine, Kyoto, Japan

†Brain Science Institute (BSI), RIKEN, Saitama, Japan

‡Department of Biochemistry and Molecular Biology, China Medical University, Shenyang, Liaoning, China

§Institute of Development, Aging and Cancer, Tohoku University, Miyagi, Japan

¶Core Research for Evolutional Science and Technology (CREST), Japan Science and Technology Corporation, Kawaguchi, Japan

Abstract

Parkin, a ubiquitin ligase, is responsible for autosomal recessive juvenile parkinsonism (AR-JP). We identified parkin-associated endothelin receptor-like receptor (Pael-R) as a substrate of parkin, whose accumulation is thought to induce unfolded protein response (UPR) -mediated cell death, leading to dopaminergic neurodegeneration. To create an animal model of AR-JP, we generated parkin knockout/Pael-R transgenic (*parkin*-ko/*Pael-R*-tg) mice. *parkin*-ko/*Pael-R*-tg mice exhibited early and progressive loss of dopaminergic as well as noradrenergic neurons without formation of inclusion bodies, recapitulating the pathological features of AR-JP. Evidence of activation of UPR and up-regulation of dopamine and its metabolites were observed throughout the lifetime. Moreover, complex I activity of mitochondria isolated from *parkin*-ko/*Pael-R*-tg mice was significantly reduced later in life. These findings suggest that persistent induction of unfolded protein stress underlies chronic progressive catecholaminergic neuronal death, and that dysfunction of mitochondrial complex I and oxidative stress might be involved in the progression of Parkinson's disease. *parkin*-ko/*Pael-R*-tg mice represents an AR-JP mouse model displaying chronic and selective loss of catecholaminergic neurons.

Keywords: dopaminergic neuron, endoplasmic reticulam stress, mitochondrial complex I, Pael-R, parkin.

J. Neurochem. (2008) **107**, 171–185.

Parkinson's disease (PD) is an age-related movement disorder including tremor, rigidity, bradykinesia and postural instability. A variety of evidence has strongly demonstrated that these motor symptoms are related to the selective degeneration of dopaminergic neurons in the substantia nigra pars compacta (SNpc) (Olanow and Tatton 1999). However, the underlying molecules and cellular pathways that mediate neuronal death remain poorly defined. Although the majority of PD cases appear to present without a family history of disease, several genes such as *α-synuclein, parkin, DJ-1, PINK-1,* and *LRRK2* have been identified as the genes responsible for familial PD. Among genes identified to date, mutations of parkin have been shown to be the cause of autosomal recessive juvenile parkinsonism (AR-JP) (Kitada *et al.* 1998; Lucking *et al.* 2000). Parkin functions as a protein-ubiquitin ligase (E3) and loss of E3 activity causes AR-JP, suggesting that substrate(s) of parkin, which cannot be properly degraded and accumulates in AR-JP patients, may cause dysfunction and eventually the death of susceptible neurons (Imai *et al.* 2000; Shimura *et al.* 2000; von Coelln *et al.* 2004a). In addition, increasing evidence suggests that partial loss of parkin E3 function resulting from S-nitrosylation or covalent modification by dopamine

Received March 6, 2008; revised manuscript received July 17, 2008; accepted July 18, 2008.

Address correspondence and reprint requests to Ryosuke Takahashi, M.D., Department of Neurology, Kyoto University Graduate School of Medicine, Shogoin, Sakyo-ku, Kyoto 606-8507, Japan.
E-mail: ryosuket@kuhp.kyoto-u.ac.jp

H.-Q.W. and Y.I. equally contributed to this work.

Abbreviations used: AR-JP, autosomal recessive juvenile parkinsonism; DOPAC, 3, 4-dihydroxyphenylacetic acid; ER, endoplasmic reticulum; HVA, homovanillic acid; LC, locus coeruleus; PD, Parkinson's disease; PDGF, platelet-derived growth factor; TH, tyrosine hydroxylase; UPR, unfolded protein response.

